

The *Arabidopsis* E3 Ubiquitin Ligase HOS1 Negatively Regulates CONSTANS Abundance in the Photoperiodic Control of Flowering ^W

Ana Lazaro,^a Federico Valverde,^b Manuel Piñeiro,^a and Jose A. Jarillo^{a,1}

^aCentro de Biotecnología y Genómica de Plantas, Instituto Nacional de Investigación y Tecnología Agraria y Alimentaria-Universidad Politécnica de Madrid, 28223 Madrid, Spain

^bInstituto de Bioquímica Vegetal y Fotosíntesis, Consejo Superior de Investigaciones Científicas y Universidad de Sevilla, 41092 Sevilla, Spain

The *Arabidopsis thaliana* early in short days6 (*esd6*) mutant was isolated in a screen for mutations that accelerate flowering time. Among other developmental alterations, *esd6* displays early flowering in both long- and short-day conditions. Fine mapping of the mutation showed that the *esd6* phenotype is caused by a lesion in the HIGH EXPRESSION OF OSMOTICALLY RESPONSIVE GENES1 (*HOS1*) locus, which encodes a RING finger-containing E3 ubiquitin ligase. The *esd6/hos1* mutation causes decreased FLOWERING LOCUS C expression and requires CONSTANS (CO) protein for its early flowering phenotype under long days. Moreover, CO and HOS1 physically interact in vitro and in planta, and HOS1 regulates CO abundance, particularly during the daylight period. Accordingly, *hos1* causes a shift in the regular long-day pattern of expression of FLOWERING LOCUS T (*FT*) transcript, starting to rise 4 h after dawn in the mutant. In addition, HOS1 interacts synergistically with CONSTITUTIVE PHOTOMORPHOGENIC1, another regulator of CO protein stability, in the regulation of flowering time. Taken together, these results indicate that HOS1 is involved in the control of CO abundance, ensuring that CO activation of FT occurs only when the light period reaches a certain length and preventing precocious flowering in *Arabidopsis*.

INTRODUCTION

The integration of complex signals from environmental and endogenous cues enables plants to time the floral transition at the most advantageous moment (Michaels, 2009; de Montaigu et al., 2010; Imaizumi, 2010; Jarillo and Piñeiro, 2011). Plants growing at northern latitudes adapt their developmental program to the varying daylengths and temperatures that occur during the year (Jackson, 2009). *Arabidopsis thaliana* is a facultative long-day (LD) plant in which flowering time is controlled by a network of six major pathways: information about daylength, low winter temperatures, and growth temperature are mediated by the photoperiod, the vernalization and the ambient temperature pathways, respectively. By contrast, the aging, the autonomous, and the gibberellin pathways act more independently of ambient conditions (Fornara et al., 2010). A potent repressor of flowering, FLOWERING LOCUS C (*FLC*), integrates signals coming from both the vernalization and the autonomous pathways (Amasino, 2010). Eventually, the whole network converges in the regulation of the floral integrators: FLOWERING LOCUS T (*FT*), TWIN SISTER OF FT (*TSF*), and SUPPRESSOR OF OVEREXPRESSION OF CONSTANS1 (*SOC1*) (Fornara et al., 2010).

The photoperiod pathway comprises several genes, including GIGANTEA (*GI*), CONSTANS (*CO*), and *FT* (Kobayashi and Weigel, 2007; Turck et al., 2008). Mutations in any of these genes cause a delay in flowering mainly under LDs, whereas their overexpression accelerates flowering independently of daylength (Turck et al., 2008). *CO* is a B-box-type protein that acts in the vascular tissue of the leaves to activate *FT* and *TSF* transcription (An et al., 2004; Jackson, 2009; Tiwari et al., 2010). *CO* may induce *FT* expression by forming a DNA binding complex with NUCLEAR FACTOR Y/HEME ACTIVATOR PROTEIN proteins (Wenkel et al., 2006; Kumimoto et al., 2010) or ASYMMETRIC LEAVES1 (*AS1*) (Song et al., 2012) and by binding the *FT* promoter directly at *CO*-responsive elements (Tiwari et al., 2010), which are functional *cis*-elements required for *FT* expression (Adrian et al., 2010). *FT* protein, and possibly *TSF*, are part of the florigen that moves to the shoot apical meristem to induce flowering in response to LDs (Corbesier et al., 2007; Jaeger and Wigge, 2007; Jang et al., 2009).

Plants have developed an intricate molecular mechanism to measure daylength based on the coincidence of an internal rhythm, set by the circadian clock, with an external cue, such as light. The ability to distinguish LDs from short days (SDs) is largely the result of the complex regulation of *CO*, both at the transcriptional and posttranslational levels, and may have arisen very early in plant evolution (Serrano et al., 2009; Valverde, 2011). Under LDs, *CO* mRNA shows two peaks of expression, the first following the expression of *GI* at the end of a LD, when plants are still exposed to light, and the second during the night. Under SDs, only the night peak of *CO* expression takes place (Suárez-López et al., 2001).

¹ Address correspondence to jarillo@inia.es.

The author responsible for distribution of materials integral to the findings presented in this article in accordance with the policy described in the Instructions for Authors (www.plantcell.org) is: Jose A. Jarillo (jarillo@inia.es).

^WOnline version contains Web-only data.

www.plantcell.org/cgi/doi/10.1105/tpc.110.081885

The precise timing of CO also requires the degradation of a family of repressors, the CYCLING DOF FACTORS (CDFs), by the F-box proteins FLAVIN BINDING, KELCH REPEAT, F-BOX1 (FKF1), ZEITLUPE (ZTL), and LOV KELCH PROTEIN2 (LKP2), in conjunction with GI (Imaizumi et al., 2005; Sawa et al., 2007; Fornara et al., 2009).

The increased expression of CO in the light under LDs but not SDs is crucial for the promotion of flowering because exposure to light is required for stabilization of CO protein (Valverde et al., 2004; Jang et al., 2008). The high CO transcript levels detected during the dark phase of both LD and SDs do not correlate with CO protein accumulation because the RING finger protein CONSTITUTIVE PHOTOMORPHOGENIC1 (COP1) promotes CO degradation in the dark (Jang et al., 2008; Liu et al., 2008b). Mutations in *COP1*, encoding a component of an ubiquitin ligase complex, cause extreme early flowering under SDs. This early flowering phenotype is largely dependent on CO activity and correlates with an increase in *FT* transcription in the *cop1* mutant (Jang et al., 2008; Liu et al., 2008b). COP1 and CO interact both in vivo and in vitro, and it has been proposed that COP1 contributes to daylength perception by reducing the abundance of the CO protein during the night (Jang et al., 2008; Liu et al., 2008b; Chen et al., 2010). However, in the morning, CO degradation occurs independently of COP1 (Jang et al., 2008). Therefore, it has been suggested that an unidentified E3 ubiquitin ligase must collaborate in CO degradation during the early part of the day to ensure that CO induction of *FT* only takes place in LDs (Jang et al., 2008).

In addition to the length of the daily light/dark periods, plants also perceive light quality. Blue and far-red light promote flowering, but red light delays it (Valverde et al., 2004). Far-red light can increase CO protein levels independently of transcription (Kim et al., 2008). Blue light mediates photoperiodic control of the floral initiation by at least three different mechanisms: First, it promotes the interaction of FKF1 and GI necessary for CDFs degradation (Sawa et al., 2007); second, the blue light receptor Cryptochrome 2 (Cry2) prevents GI and CO proteolysis by COP1 (Liu et al., 2008b; Yu et al., 2008; Zuo et al., 2011); and third, Cry2 modulates *FT* transcription directly (Liu et al., 2008a). Moreover, the red light photoreceptor phytochrome B (phyB) has been implicated in the degradation of CO during the first part of the day (Valverde et al., 2004; Jang et al., 2008).

Genetic screens devoted to the isolation of early flowering mutants have revealed the existence of genes that repress the floral transition (Pouteau et al., 2004). Floral repressors are essential to safeguard against premature flowering, and knowledge of how these repressors interact with the floral promotion pathways is just emerging (Pouteau et al., 2004; Roux et al., 2006; Jarillo and Piñeiro, 2011). Here, we demonstrate that the *early in short days6* (*esd6*) early flowering mutant is caused by a lesion in the *HOS1* gene. *HOS1* encodes a protein with E3 ubiquitin ligase activity, previously described as a regulator of cold acclimation responses (Lee et al., 2001; Dong et al., 2006a). The early flowering phenotype of *hos1* is completely suppressed by *co* mutations in the Landsberg *erecta* (*Ler*) background and notably delayed by *co* mutations in the Columbia (*Col*) background. Moreover, we show that HOS1 physically interacts with CO in vitro and in planta and regulates CO protein abundance during the daylight period, indicating the participation of another

RING finger-containing protein, in addition to COP1, in the photoperiodic control of flowering time in *Arabidopsis*. Thus, we propose that HOS1 is required to modulate precisely the timing of CO accumulation and that this regulation is essential to maintain low levels of *FT* during the first part of the day and, subsequently, a correct photoperiodic response in *Arabidopsis*.

RESULTS

The *esd6* Mutant Is Early Flowering and Displays Pleiotropic Defects in Both Vegetative and Reproductive Development

A recessive mutation that accelerated flowering time, named *esd6*, was identified by screening a *Ler* mutagenized population. Plants homozygous for *esd6* were selected as early flowering under LD conditions, although the *esd6* mutation also accelerated flowering under noninductive SD photoperiods (Figures 1A and 1B, Table 1). Earliness of *esd6* was mainly associated with the production of fewer leaves during the adult vegetative phase (Figure 1D) based on leaf trichome distribution (Teifer et al., 1997).

Besides the flowering phenotype, *esd6* mutant plants also displayed complex pleiotropic alterations of both vegetative and reproductive development. Mutant plants were smaller than the wild type (Figures 1A and 1B) and showed reduced leaf size compared with *Ler* (Figure 1E). Moreover, *esd6* primary root was shorter and produced fewer secondary roots than the wild type (Figure 1G; see Supplemental Figure 1 online). By contrast, stem length was not noticeably affected by the *esd6* mutation (Figure 1C). *esd6* flowers also displayed some developmental abnormalities, including a reduced flower size in comparison to the wild type (Figure 1F; see Supplemental Figure 1 online). In addition, siliques were ~30% shorter in *esd6* mutant than in *Ler* (Figure 1F; see Supplemental Figure 1 online).

Because the *esd6* mutant looked paler than *Ler*, we decided to measure the total chlorophyll content present in both genotypes (Figure 1H). We included *phyB-1* as a control in this experiment, since *phyB* mutants display reduced chlorophyll accumulation (Reed et al., 1993). As expected, both *phyB-1* and *esd6* mutants showed less chlorophyll than *Ler* (Figure 1H), indicating an additional role of *ESD6* gene in the regulation of chlorophyll biosynthesis.

The *ESD6* Gene Encodes HOS1, an E3 Ubiquitin Ligase

esd6 was identified in a *Ler* transposon-mutagenized population generated from the cross between two transgenic *Ler* plants, one containing the *Dissociation* (*Ds*) element and the other the transposase gene, capable of mobilizing the *Ds* element. The *esd6* mutant was selected in the F2 population where plants with different phenotypes were observed due to the mobilization of the transposon. The *esd6* early flowering phenotype did not cosegregate with the selection resistance gene. For this reason, we considered that the mutation originated from a second mobilization event of the *Ds* element that left a fingerprint in the genome. Consequently, to understand the molecular function of *ESD6*, we performed a map-based cloning approach. *ESD6* was initially located in the upper arm of chromosome 2, and further

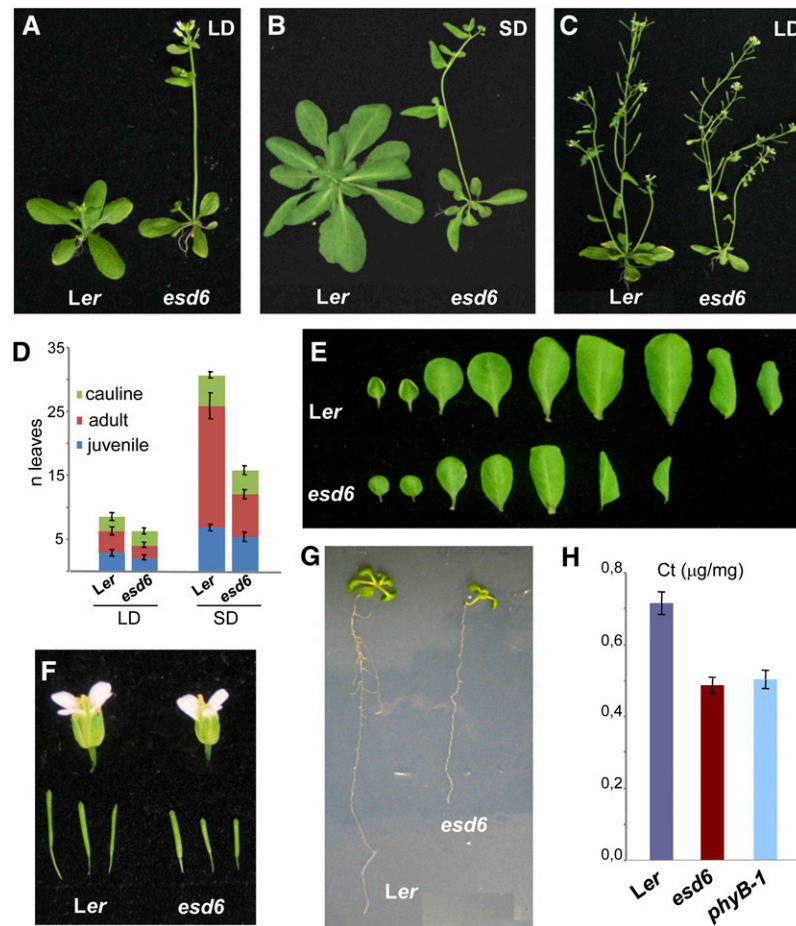


Figure 1. Phenotypic Characterization of the *esd6* Mutant.

- (A) and (B) Flowering time phenotype of *Ler* and *esd6* plants grown in LD conditions for 23 d (A) or in SD conditions for 54 d (B).
 (C) Phenotype of *Ler* and *esd6* plants grown in LD conditions for 35 d.
 (D) Histograms comparing the number of juvenile, adult, and cauline leaves in *Ler* and *esd6* plants grown under both LD and SD photoperiods.
 (E) Rosette and cauline leaves of *Ler* and *esd6* plants grown in LDs.
 (F) Detached *Ler* and *esd6* flowers and siliques from plants grown under LD conditions.
 (G) Root elongation in 11-d-old *Ler* and *esd6* seedlings.
 (H) Total chlorophyll content (Ct) in *Ler* and *esd6* and *phyB-1* mutant seedlings.

linkage analyses allowed us to define a candidate region between C005 and T517 molecular markers (see Supplemental Table 1 online), which encompassed eight open reading frames (see Supplemental Figure 2 online). Among these loci, *HOS1* (*At2g39810*) had already been described as a regulator of cold acclimation responses also affecting flowering time (Lee et al., 2001). The sequencing of this transcription unit in *esd6* revealed a single nucleotide deletion in the position 2212 (fifth exon), which generated a premature stop codon (Figure 2A). To confirm that *esd6* was indeed affecting the same locus as the *hos1-1* mutation, we performed an allelism test. The F1 plants derived from the cross between *hos1-1*, in C24 background, and the *esd6* mutant were early flowering, indicating that the two mutations were allelic (Table 1). The *esd6* mutant will be referred to hereafter as *hos1-2*. In addition, we searched for T-DNA insertion alleles within the *HOS1* locus and identified the line

SALK_069312, which carried an insertion in the fifth exon of the *HOS1* gene (Figure 2A). This T-DNA mutant allele was named *hos1-3*, and an additional allele, *hos1-4*, was obtained later on in our laboratory during the screening of an ethyl methanesulfonate-mutagenized population of *Col* plants. The *hos1-4* mutation is a deletion of nucleotide 88 from the annotated translational start of *HOS1* that generates a premature stop codon in the first exon of the gene (Figure 2A). All *hos1* alleles analyzed display an early flowering phenotype both in LD and SD photoperiods, but the fact that they flower earlier under inductive photoperiods indicates that the mutation does not completely abolish the plant photoperiod response (Figure 2B, Table 1).

The *HOS1* gene is around 5.5 kb long, bears nine exons, and encodes a protein of 915 amino acids that contains a noncanonical RING finger domain in the N-terminal region and a putative nuclear localization signal in the C-terminal part (Figure 2A; see

Table 1. Flowering Time of *hos1* Double Mutants

Genotype	LD	SD
C24	25.6 ± 3.7	56.3 ± 7.2
<i>hos1-1</i> (C24)	11.9 ± 2.2	38.7 ± 7.0
<i>Ler</i>	8.4 ± 0.9	24.1 ± 3.3
<i>hos1-2</i> (<i>Ler</i>)	6.7 ± 0.9	17.6 ± 1.9
<i>Col</i>	13 ± 1.1	71.8 ± 6.5
<i>hos1-3</i> (<i>Col</i>)	7.2 ± 0.5	32.5 ± 6
<i>hos1-1</i> × <i>hos1-2</i> (<i>F1</i>)	8.1 ± 1	n.d.
<i>flc-3</i> (<i>Col</i>)	9.1 ± 0.6	61.9 ± 12.7
<i>hos1-3 flc-3</i>	6.8 ± 0.4	33.7 ± 6.7
<i>Col FRI Sf-2</i>	61.7 ± 9.6	121.3 ± 21.6
<i>hos1-3 FRI Sf-2</i>	40.9 ± 6.8	129.9 ± 16.4
<i>fca-1</i> (<i>Ler</i>)	33.3 ± 4.5	84.6 ± 11.2
<i>hos1-2 fca-1</i>	15.4 ± 1.8	79.9 ± 10.8
<i>fve-3</i> (<i>Col</i>)	42.8 ± 6.1	108.4 ± 11.8
<i>hos1-3 fve-3</i>	13.6 ± 1.1	94.6 ± 9.2
<i>fld-1</i> (<i>Col</i>)	36.6 ± 6	117.2 ± 8.5
<i>hos1-3 fld-1</i>	16.8 ± 3.3	110.4 ± 4.9
<i>siz1-2</i> (<i>Col</i>)	10.2 ± 1.1	16 ± 2.3
<i>hos1-3 siz1-2</i>	7.4 ± 0.6	13.7 ± 3.1
<i>fha-1</i> (<i>Ler</i>)	12.5 ± 0.8	n.d.
<i>hos1-2 fha-1</i>	8.7 ± 0.8	n.d.
<i>gi-3</i> (<i>Ler</i>)	25 ± 2	n.d.
<i>hos1-2 gi-3</i>	18.6 ± 1.2	n.d.
<i>co-2</i> (<i>Ler</i>)	21.8 ± 5.9	23.4 ± 2.7
<i>hos1-2 co-2</i>	20.1 ± 1.3	14 ± 2.2
<i>co-10</i> (<i>Col</i>)	38.6 ± 10.9	n.d.
<i>hos1-3 co-10</i>	26 ± 6.9	n.d.
<i>cop1-4</i> (<i>Col</i>)	11.8 ± 0.9	12.8 ± 1.6
<i>hos1-3 cop1-4</i>	5 ± 0.6	5.1 ± 1
<i>cop1-4 co-10</i>	28.9 ± 4.2	n.d.
<i>hos1-3 cop1-4 co-10</i>	20.3 ± 3.2	n.d.
<i>fkf1-1</i> (<i>Col</i>)	46.1 ± 6.1	n.d.
<i>hos1-3 fkf1-1</i>	17.5 ± 1.8	n.d.
<i>Col</i> (35S:CO)	4 ± 0	n.d.
<i>hos1-3</i> (35S:CO)	4.1 ± 0.3	n.d.
<i>ft-1</i> (<i>Ler</i>)	17.3 ± 1.9	39.2 ± 4.8
<i>hos1-2 ft-1</i>	16.7 ± 0.8	35.9 ± 2.9
<i>soc1-1</i> (<i>Ler</i>)	14 ± 1.9	56.2 ± 5.3
<i>hos1-2 soc1-1</i>	10.2 ± 0.6	30.2 ± 5.4
<i>ft-1 soc1-1</i>	37.2 ± 3.3	n.d.
<i>hos1-2 ft-1 soc1-1</i>	32.6 ± 2.9	n.d.

Total number of leaves at the time of flowering for the different wild-type ecotypes and single, double, and triple mutants described in this work. Data were scored in approximately 30 plants under LD conditions and 15 plants under SD photoperiods and are represented as mean ± SD. n.d., not determined.

Supplemental Figure 3 online). *HOS1* is a unique gene in *Arabidopsis*, and putative orthologs have only been found in plants. The Cys residues present in the RING finger domain are totally conserved between all *HOS1* orthologs (see Supplemental Figure 3 online). RING finger domains are found in proteins with E3 ubiquitin ligase activity that participate in the ubiquitin/26S proteasome pathway (Deshaies and Joazeiro, 2009; Vierstra, 2009). Previously, it was shown that *Arabidopsis* *HOS1* can function as an E3 ubiquitin ligase in ubiquitination assays (Dong et al., 2006a).

hos1 Mutations Affect *FLC* Expression and Have an *FLC*-Independent Effect in the Control of Flowering Time

The early flowering phenotype of *hos1* mutants suggested that *HOS1* could be a negative regulator of the floral transition in *Arabidopsis*. To test this hypothesis, we analyzed the phenotype of double mutants carrying *hos1* and different mutations affecting flowering time. It had been previously described that *FLC* expression levels were reduced in the *hos1-1* mutant compared with C24 accession (Lee et al., 2001). In order to check if the *hos1* early flowering phenotype was fully dependent on *FLC*, the effect of the *hos1-3* mutation in an *flc* null genetic background (*flc-3*) (Michaels and Amasino, 1999) was tested. Both *hos1-3* and *hos1-3 flc-3* double mutant plants flowered with the same number of leaves, irrespectively of photoperiodic conditions, although the *hos1-3 flc-3* plants bolted consistently earlier than *hos1-3* under LD (Figure 3A, Table 1). This result may indicate that there is no additional effect of *flc* null mutation on the acceleration of flowering time caused by *hos1*. Besides, both *hos1-3* and *hos1-3 flc-3* plants flowered clearly earlier than *flc-3* plants under both LD and SD conditions (Figure 3A, Table 1), indicating that the effect of the *hos1* mutation on flowering time could not be exclusively dependent on *FLC* activity and that there is an *FLC*-independent effect responsible for the early flowering phenotype of *hos1*. To find out whether *FLC* expression was altered in the *hos1* mutant alleles isolated in different backgrounds, RT-PCR analyses were performed in *hos1-1*, *hos1-2*, and *hos1-3* mutants and the corresponding wild-type genotypes. Consistent with previous results (Lee et al., 2001), in all *hos1* mutants assayed, *FLC* transcript was clearly downregulated (Figure 3B); therefore, it cannot be ruled out that this change in *FLC* expression has an effect on the early flowering time of the *hos1* alleles.

Dominant alleles of *FRIGIDA* (*FRI*) confer a vernalization requirement that delays flowering through the upregulation of *FLC* (Johanson et al., 2000). To find out the genetic relationship between *HOS1* and *FRI*, the mutant *hos1-3* was crossed with a *Col* plant bearing an active *FRI* allele introgressed from the San Feliu-2 (*Sf-2*) accession (Lee and Amasino, 1995). Under LD conditions, the *hos1-3 FRI Sf-2* line showed an additive phenotype, the *FRI* late-flowering phenotype being only partially suppressed by *hos1-3* (Figure 3D, top panel, Table 1). This suggests that *HOS1* and *FRI* do not regulate *FLC* expression through the same pathway in LDs. By contrast, the *hos1-3 FRI Sf-2* plant flowered with approximately the same number of leaves as the *Col FRI Sf-2* plants under SD conditions, abolishing the effect of the *hos1* mutation (Figure 3D, bottom panel, Table 1).

Because *HOS1* is involved in cold signal transduction (Lee et al., 2001) and vernalization regulates *FLC* expression (Amasino, 2010), we hypothesized that *HOS1* could be controlling *FLC* transcript levels through the vernalization pathway. To analyze this, we generated combinations between *hos1* and two other mutants impaired in the vernalization response, *vernalization1* (*vm1*) and *vernalization-insensitive3* (*vin3*) (Levy et al., 2002; Sung and Amasino, 2004), both in late flowering backgrounds that allowed us to observe the acceleration of flowering due to the vernalization treatment. The *hos1* mutation did not impair

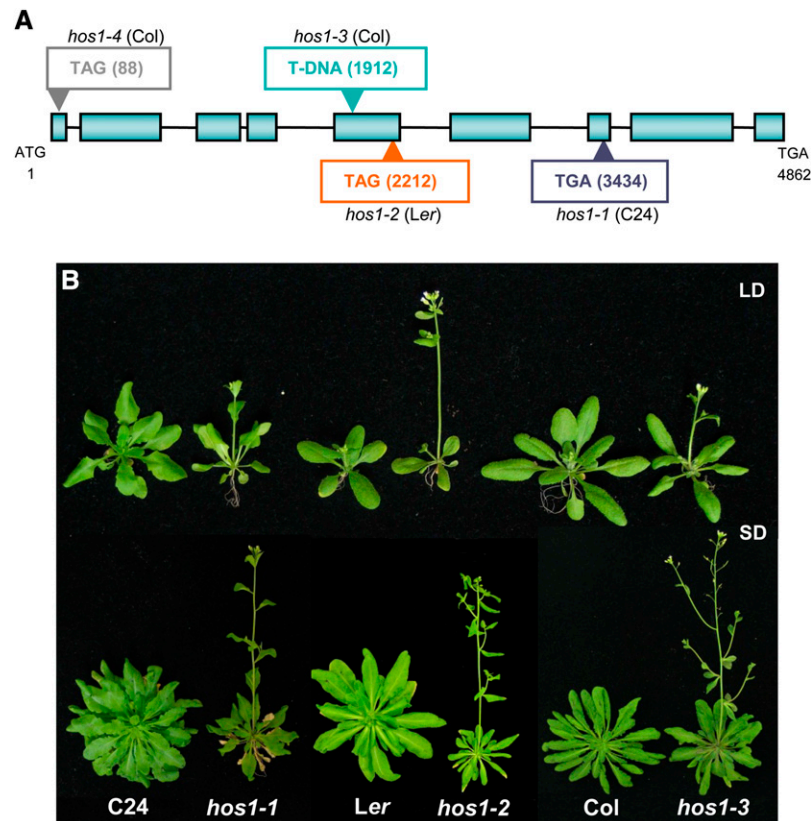


Figure 2. *ESD6* Encodes *HOS1*.

(A) *ESD6/HOS1* gene structure showing the mutations present in the different *hos1* alleles. Exons are represented by boxes and introns by a line. **(B)** Pictures illustrating the flowering time of *hos1* mutants and their respective wild-type genotypes in LD and SD conditions. Plants were grown for 23 d under LD conditions (Top). SD pictures (Bottom) were taken after 64 d for C24 and *hos1-1*, 58 d for *Ler* and *hos1-2*, and 60 d for *Col* and *hos1-3*.

the acceleration of flowering caused by vernalization when combined with the late flowering *fca-1* or *FRI* Sf-2 plants (see Supplemental Table 2 online). Besides, no difference in flowering time was found for the *hos1-2 vrn1-2 fca-1* triple mutant grown after either 1 or 4 weeks of vernalization treatment (see Supplemental Table 2 online). The same result was observed for *hos1-3 vin3-4* carrying an active *FRI* allele, as both 1- and 4-week-vernalized plants flowered with approximately the same number of leaves (see Supplemental Table 2 online). Thus, we conclude that *HOS1* does not regulate *FLC* expression through the vernalization pathway.

Considering that the autonomous pathway also converges on the regulation of *FLC* expression, the flowering phenotype of double mutants combining *hos1* and mutations in representative autonomous pathway genes was analyzed, in particular the *hos1-3 five-3*, *hos1-2 fca-1*, and *hos1-3 fld-1* double mutants. Under LD, these double mutant plants showed an additive phenotype because the late-flowering phenotype of autonomous pathway mutants was only partially suppressed by *hos1* (Figure 3C, top panel, Table 1). By contrast, under SDs, flowering time of these double mutants was very similar to the one displayed by the autonomous pathway mutants, as they pro-

duced only a few leaves less than *five-3*, *fca-1*, and *fld-1* respectively (Figure 3C, bottom panel, Table 1).

Altogether, these results indicate that the *hos1* mutation cannot accelerate flowering in SDs when combined with genetic backgrounds that have very high *FLC* expression levels, such as mutations of the autonomous pathway or active alleles of *FRI*. By contrast, under LDs, the repressive effect of *HOS1* on flowering time may be mediated by additional pathways that remain inactive in SDs.

The E3 SUMO ligase *SIZ1* promotes *FLC* expression by repressing the autonomous pathway gene *FLD* (Jin et al., 2008). Besides, *SIZ1* stabilizes the *ICE1* protein, which has been implicated in the regulation of freezing tolerance in *Arabidopsis* (Miura et al., 2007). Because it had been described that *ICE1* was also targeted by *HOS1* (Dong et al., 2006a), we checked the genetic relationship between *hos1* and *siz1* mutants. Flowering time of *siz1* plants relative to the wild type was slightly earlier under LDs and substantially earlier under SDs (Jin et al., 2008) (Table 1). When we combined *siz1-2* with the *hos1-2* mutation, the double mutant flowering time resembled that of *hos1-2* in LDs but was earlier than any of the parental lines in SDs, suggesting a synergistic genetic interaction between both loci (Table 1).

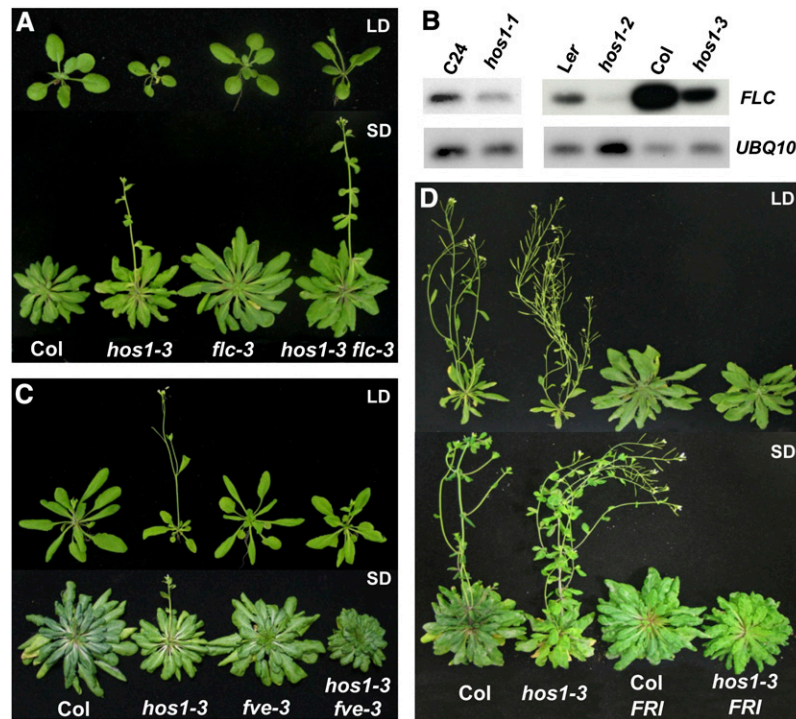


Figure 3. *hos1* Mutations Downregulate *FLC* Expression and Have an *FLC*-Independent Effect in the Control of Flowering Time.

(A) Flowering time phenotype of *hos1-3 flc-3* double mutant in LD (**Top**) and SD (**Bottom**) conditions.

(B) Analysis of the expression of *FLC* in 14-d-old *hos1* mutant seedlings and their corresponding wild-type genotypes. *FLC* expression was monitored by RT-PCR using 22 cycles for C24 and *hos1-1* and 28 cycles for *Ler*, *hos1-2*, *Col*, and *hos1-3*. For the *UBQ10* control, 22 cycles were used.

(C) Flowering time phenotype of *hos1-3 fve-3* double mutant plants grown in LD (**Top**) and SD (**Bottom**) conditions.

(D) Flowering time phenotype of *hos1-3* plants bearing an active allele of *FRI* in LDs (**Top**) and SDs (**Bottom**).

The Early Flowering Phenotype of *hos1-2* Requires a Functional *CO* Gene

We also analyzed the phenotype of double mutants carrying *hos1* and mutations in genes representative of the photoperiod pathway, such as *CRY2/FHA*, *GI*, and *CO*, which delay flowering mainly under LDs (Koorneef et al., 1998). While *hos1-2 fha-1* and *hos1-2 gi-3* double mutants showed an additive flowering phenotype between *hos1-2* and *fha-1* and *gi-3* late flowering mutants, the genetic interaction observed between *hos1-2* and *co-2* was completely different (Figure 4, Table 1). Under LDs, the *hos1-2* mutation did not accelerate flowering time when it was combined with *co-2* (Figure 4C, Table 1); indeed, *hos1-2 co-2* plants flowered with the same number of leaves as *co-2* mutants, indicating that the early flowering phenotype of *hos1-2* has a strong requirement for a functional *CO* gene. However, under SD conditions, *hos1-2 co-2* flowered as early as *hos1-2* (Table 1), given that *co* mutations do not delay flowering under this photoperiodic condition. These genetic results suggest that *HOS1* is involved in the photoperiodic control of flowering time as a negative regulator of *CO* under LDs.

FKF1 is an F-box protein (Imaizumi et al., 2005) that mediates the cyclic degradation of CDF proteins, which are repressors of *CO* expression (Imaizumi et al., 2005; Fornara et al., 2009). To study if there was any genetic interaction between *FKF1* and

HOS1, the double mutant *hos1-3 fkf1-1* was analyzed and it showed an additive phenotype between the late flowering time of *fkf1-1* and the early flowering phenotype of *hos1-3* in LDs (Table 1). This result indicates that *HOS1* does not participate in the *FKF1* transcriptional regulatory pathway that controls *CO* expression.

hos1 Mutants Show an Altered Pattern of *FT* Expression

FLC represses the expression of the floral integrators *FT* and *SOC1*, while the photoperiod pathway activates *FT* and *SOC1* expression through *CO* (Yoo et al., 2005; Searle et al., 2006; Turck et al., 2008). Because *hos1* mutations showed downregulation of *FLC* expression (Figure 3B) and the *co-2* mutation was epistatic to *hos1-2* under LDs (Figure 4C), we decided to check the genetic relationship between *HOS1* and the floral integrators *FT* and *SOC1*. The *hos1-2 ft-1* double mutant showed a similar flowering phenotype to *ft-1* under LD conditions, suggesting a strong requirement for *FT* for the *hos1* early flowering phenotype (Figure 5A, Table 1). By contrast, the *hos1-2 soc1-1* double mutant was additive between the parental lines in both LD and SD conditions (Figure 5A, Table 1). This result is in accordance with the epistasis observed between *co-2* and *hos1-2*, considering that *FT* is the main target of *CO* under LDs (Yoo et al., 2005). To check whether the whole effect of *HOS1* on flowering time was through *FT* and *SOC1*, we generated the triple

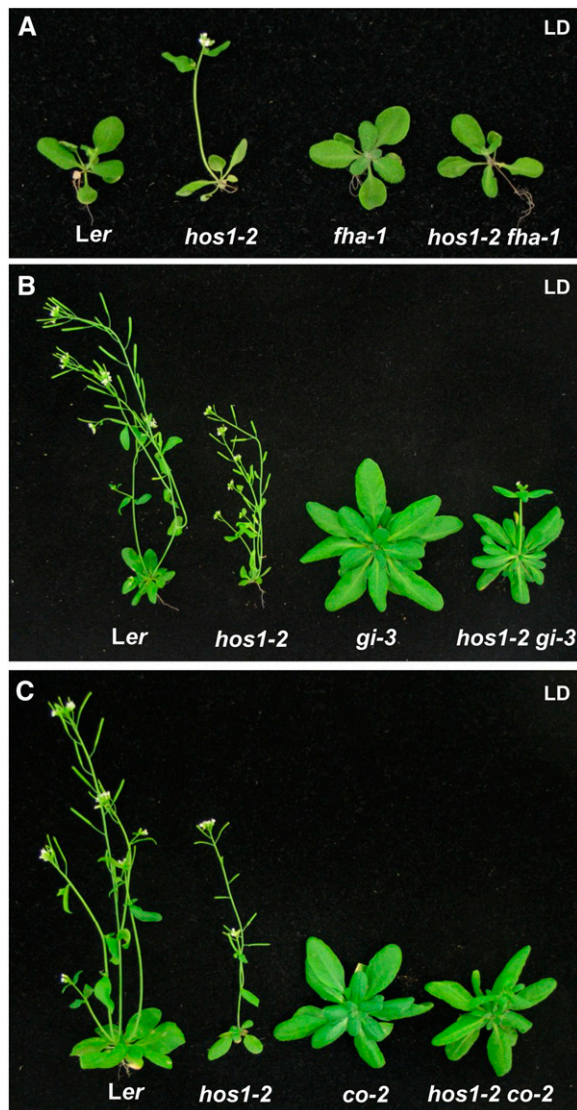


Figure 4. Genetic Analyses of *hos1* and Mutations in Photoperiod Pathway Genes.

Flowering time phenotype of *hos1-2 fha-1* (A), *hos1-2 gi-3* (B), and *hos1-2 co-2* (C) double mutants grown in LD conditions. Pictures were taken after 22, 43, and 38 d, respectively.

mutant *hos1-2 ft-1 soc1-1*. Flowering time analysis showed that the triple mutant was slightly earlier than *ft-1soc1-1* (Figure 5A, Table 1). This result indicates that the early flowering phenotype of *hos1* mutation requires functional *FT* and *SOC1* genes, although we cannot rule out that *HOS1* could regulate other protein(s) involved in the control of flowering time.

To deepen our understanding of the genetic relationship observed between *HOS1* and the photoperiod pathway, we performed a time course expression analysis over a 24-h period in *Ler* and *hos1-2* seedlings both in LDs and SDs. First of all, we demonstrated that *HOS1* transcript did not show a diurnal oscillation in *Ler* background (Figure 5B). Next, we analyzed

the temporal expression pattern of *CO*, *FT*, and *SOC1* genes using RT-PCR (see Supplemental Figure 4 online) and quantitative real-time PCR (Q-PCR) (Figures 5C and 5D) approaches. As previously reported, *CO* transcript level in *Ler* background was high at dawn and dusk and during the night, remaining low for the rest of the light period of the day (Suárez-López et al., 2001). In *hos1-2*, the same pattern of *CO* expression was observed, indicating that *hos1* mutation did not affect significantly the levels or the expression profile of the *CO* transcript (Figures 5C and 5D). However, the expression pattern of the floral integrator *FT* was clearly altered in the *hos1-2* mutant compared with the wild type both in LD and SD conditions (Figures 5C and 5D). *FT* transcript usually shows a peak of expression at dusk in LDs (around zeitgeber time (ZT) 16), following the evening increase observed in *CO* mRNA. In the *hos1-2* mutant, a peak of *FT* expression in the subjective morning, mainly at ZT4, but also at ZT8 was observed, when the *CO* transcript levels are barely detectable in the mutant (Figure 5C). To check whether this alteration was due to a specific developmental stage of the plant or if it relied on the genetic background, *FT* transcript levels were analyzed at ZT4 and ZT8 in *Col* and *hos1-3* plants harvested 8, 10, 12, and 15 d after germination. In every single stage tested, *FT* expression was higher in *hos1-3* in relation to *Col* in the first part of the day (see Supplemental Figure 5 online). In SDs, an increased *FT* expression in the *hos1-2* mutant, starting to rise at ZT8 and peaking at ZT12 was observed, which may explain the early flowering phenotype displayed by the mutant under non-inductive photoperiods (Figure 5D). A small but consistent increase in *SOC1* expression was also detected in *hos1-2* plants grown in LD photoperiods in comparison to the wild type (Figure 5C). Thus, we conclude that *CO* transcript levels are not modified substantially by the *hos1* mutation and that *HOS1* is required to repress the expression of *FT* in the first part of the day in LD. Considering that *HOS1* has an E3 ubiquitin ligase activity, we speculated that it may be involved in the degradation of proteins that regulate *FT* expression. Both the genetic analysis and the expression assays suggested that this protein could be *CO*.

HOS1 Interacts in Vitro and in Vivo with CO and Regulates Its Abundance

Given the proposed epistatic interaction between *co-2* and *hos1-2* mutants and considering that *CO* transcript levels were not affected in the *hos1-2* mutant, we decided to analyze whether there was a physical interaction between *CO* and *HOS1*. For this purpose, we conducted in vitro pull-down experiments using Maltose Binding Protein (MBP)-*HOS1* and in vitro-translated *CO* protein. As shown in Figure 6A, MBP-*HOS1*, but not MBP alone, was able to interact with *CO* protein. Whether the interaction between *CO* and *HOS1* also occurred in vivo was tested using bimolecular fluorescence complementation (BiFC). For BiFC, the N terminus of yellow fluorescent protein (YFP) was cloned upstream of *HOS1* (YFN-*HOS1*), and the C terminus of YFP was fused to *CO* (YFC-*CO*). By *Agrobacterium tumefaciens* coinfiltration, these constructs were transiently expressed in abaxial epidermal cells of tobacco (*Nicotiana benthamiana*) and *Arabidopsis* leaves (Voinnet et al., 2003). Reconstitution of YFP fluorescence was examined by confocal microscopy 2 d after

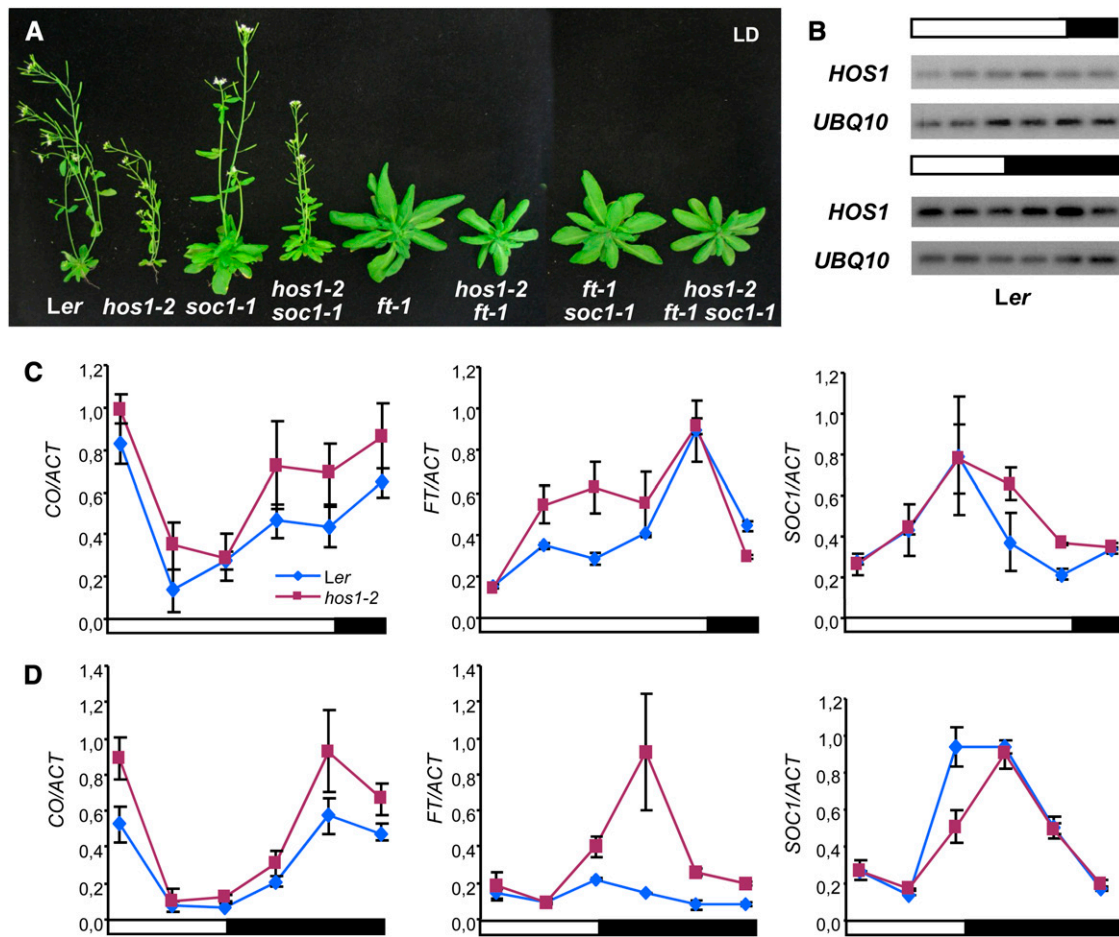


Figure 5. The Early Flowering Phenotype of *hos1* Depends on FT and SOC1 Functional Proteins and *hos1* Mutation Alters the Pattern of Expression of *FT*.

(A) Flowering time phenotype of *hos1-2 soc1-1*, *hos1-2 ft-1*, and *hos1-2 ft-1 soc1-1* triple mutant plants grown in LD conditions.
(B) *HOS1* expression pattern over a 24-h time course in *Ler* seedlings grown for 8 d in LDs and for 16 d in SDs. Samples were harvested every 4 h after dawn. *HOS1* expression was monitored by RT-PCR using 20 cycles.
(C) and **(D)** Expression analysis of different flowering time genes over a 24-h time course in *Ler* and *hos1-2* seedlings grown for 8 d in LDs and 16 d in SDs.
(C) Samples were harvested every 4 h after dawn. Q-PCR analysis of *CO*, *FT*, and *SOC1* expression in LD conditions.
(D) Same as **(C)** but *Ler* and *hos1-2* seedlings grown in SD conditions. Relative expression levels were normalized to *ACT2* expression.

transient coexpression of the protein pairs. Yellow fluorescence in the nucleus was detected with coexpression of YFC-CO and YFN-HOS1, but no yellow fluorescence was observed when YFC-CO was coexpressed with YFN-AKIN β or when YFC-AKIN10 was coexpressed with YFN-HOS1, as negative controls (Figure 6B). As a positive control, the interaction between amino and carboxy parts of AKIN β and AKIN10 Sucrose nonfermenting1 (SNF1)-related protein kinases (Ferrando et al., 2001) was tested (Figure 6B). The CO-HOS1 interaction was observed in conspicuous nuclear speckles, which have been often associated with foci of proteasome degradation, as previously described for the interaction between CO and COP1 (Jang et al., 2008). These results demonstrate that CO and HOS1 colocalize and physically interact in the nuclei of plant cells.

The interaction between HOS1 and CO proteins was further explored by in vivo coimmunoprecipitation analysis. For this experiment, we generated *35S:HOS1-GFP* (for green fluorescent protein) transgenic plants in *Col* background, and we also introduced this construct into *35S:CO* plants. Nuclear proteins isolated from 2-week-old *35S:HOS1-GFP 35S:CO* and *35S:HOS1-GFP* plants, grown in LD and harvested at ZT4 in the presence of MG132 proteasome inhibitor, were immunoprecipitated after incubation with an anti-GFP antibody (Figure 6C). The eluted purified proteins were blotted and detected with anti-CO antibody. As shown in Figure 6C, CO antibody recognized a clear signal in nuclear extracts from *35S:HOS1-GFP 35S:CO* (Figure 6C, elution HC, marked by an arrow) plants but not in control extracts from the *35S:HOS1-GFP* (Figure 6C, elution H) plants.

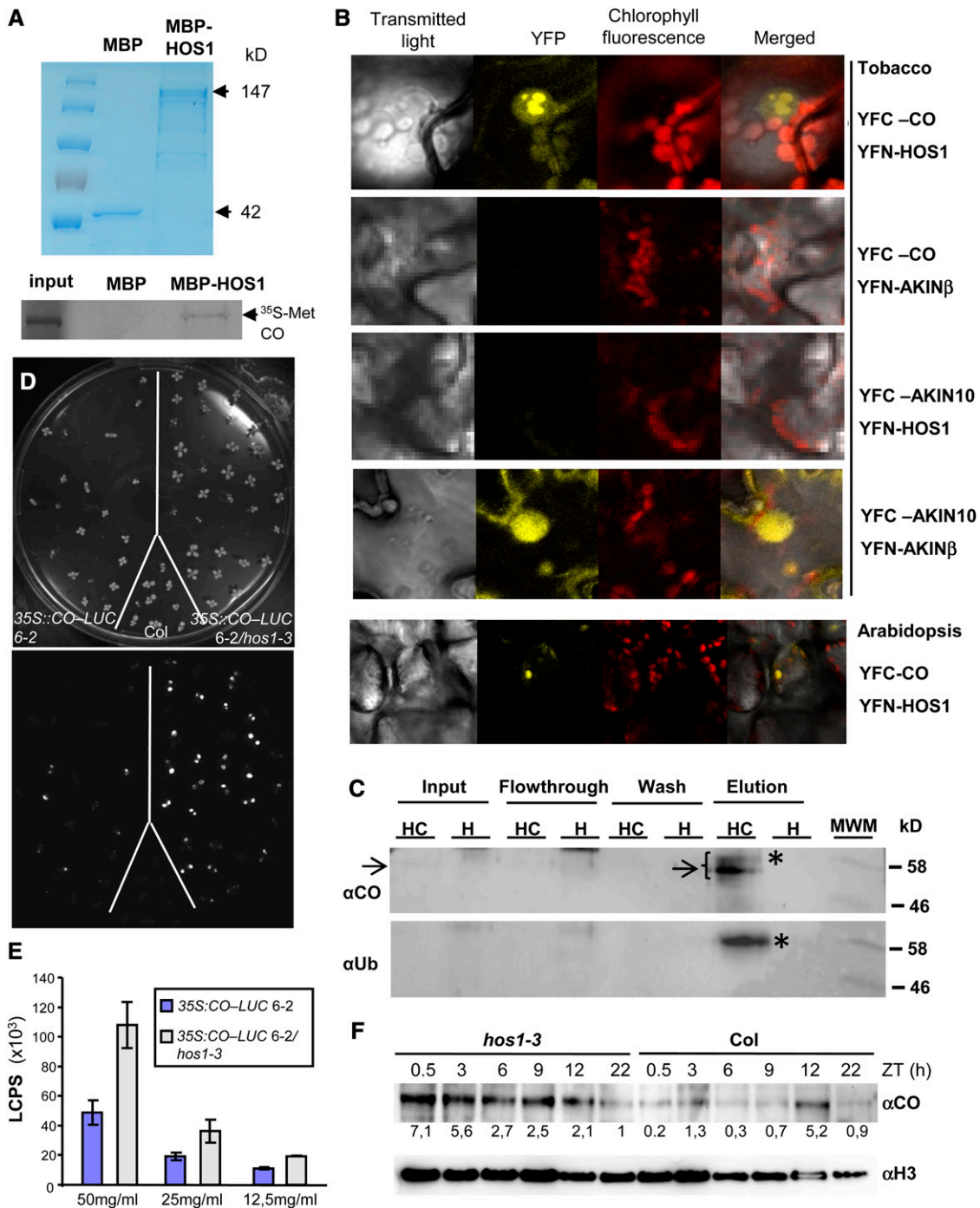


Figure 6. HOS1 Interacts with CO and Regulates Its Abundance.

(A) HOS1 and CO interact in vitro. A Coomassie blue-stained SDS-PAGE showing MBP (42 kD) and MBP-HOS1 fusion protein (147 kD) expressed in *E. coli* BL21 Rosetta strain and purified on amylose resin is shown in the top panel. The bottom panel shows the result of a pull-down assay with MBP and MBP-HOS1 proteins incubated with [³⁵S]Met-labeled CO protein. Retained CO protein was visualized after autoradiography of the dried gel.

(B) HOS1 interacts with CO in planta. BiFC assay coexpressing the C terminus of YFP fused to CO (YFC-CO) and the N terminus of YFP to HOS1 (YFN-HOS1) in tobacco and *Arabidopsis* leaves. Yellow fluorescence in the nucleus indicated interaction. Negative and positive controls were included in the assay.

(C) In vivo coimmunoprecipitation between HOS1 and CO. GFP-HOS1 protein was immunoprecipitated from 35S::GFP-HOS1 35S::CO (HC) and 35S::GFP-HOS1 (H) plants employing GFP antibody-agarose columns and detected with anti-CO antibodies (elution HC, Top). The arrow marks both the

Given their apparent molecular mass and the comigration with the input CO protein (Figure 6C, marked with an arrow), which included 1/50 protein amount of the immunoprecipitated fraction (Figure 6C, input HC), the recognized bands must correspond to CO protein. In this blot, a higher molecular mass CO form (Figure 6C, asterisk, top panel) could also be detected. Because HOS1 has been described as a RING finger E3 ligase (Dong et al., 2006a), the same blot was probed with antiubiquitin antibody, which detected only the upper immunoprecipitated band (Figure 6C, asterisk, bottom panel). This result demonstrates that a fraction of the immunoprecipitated CO protein was ubiquitinated *in vivo*, further supporting the association between both proteins and pointing to a role of HOS1 in the proteasome-dependent degradation of CO.

It has been reported that HOS1 has autoubiquitination ligase activity *in vitro* and that it can also mediate the ubiquitination and degradation of ICE1 transcription factor (Dong et al., 2006a). To further analyze whether HOS1 may also regulate CO degradation *in vivo*, a construct constitutively expressing CO fused to luciferase (*LUC*) was transformed into wild-type *Arabidopsis* plants. One representative line, 35S:CO-LUC 6-2, displaying an early flowering phenotype, was crossed into *hos1-3*. The 35S:CO-LUC 6-2/*hos1-3* plants flowered earlier than either the *hos1-3* mutant or the 35S:CO-LUC 6-2 plants, indicating that the CO-LUC construct was fully functional (see Supplemental Table 3 online). Using *in vivo* imaging of *LUC* fluorescence, we found that under LDs the CO protein levels were substantially lower in the wild type than in the *hos1* mutant background three hours after dawn (ZT3) (Figure 6D), suggesting that the degradation of CO that occurs in the wild type is impaired in the *hos1* mutant. Quantification of *LUC* activity corroborated that CO protein accumulated to higher levels in the *hos1* mutant than in the wild-type plants (Figure 6E). This accumulation of CO protein observed at ZT3 correlates with the early peak of *FT* expression present in the *hos1* mutant (Figures 5C and 5D; see Supplemental Figure 4 online). To further assess the role of HOS1 in CO regulation, we performed immunoblot assays to detect CO protein in nuclear extracts from wild-type and *hos1-3* plants grown under LD photoperiods. In these immunoblots, CO protein was present at lower abundance in the wild type than in the *hos1-3* mutant plants, particularly during the daylight period (Figure 6F). From these data, we conclude that HOS1 is involved in the photoperiodic regulation of flowering through the modulation of CO protein levels *in vivo*.

HOS1 Is a Nuclear-Localized Protein That Acts in the Phloem to Regulate Photoperiodic Flowering

HOS1 protein is ubiquitously expressed in all plant tissues (Lee et al., 2001). Computer analysis of the HOS1 amino acid sequence predicted a nuclear localization signal in the C terminus of the protein (see Supplemental Figure 3 online). Previous reports localized HOS1 into the cytoplasm of transgenic *Arabidopsis* seedlings overexpressing a *HOS1-GFP* construct, grown under dark conditions at normal growth temperature. However, in response to low temperature treatments, HOS1-GFP accumulated in the nucleus (Lee et al., 2001). To determine whether the subcellular localization of HOS1 was altered by light/dark conditions, we overexpressed a *HOS1-GFP* construct in the *hos1-3* mutant. The homozygous line 35S:HOS1-GFP/*hos1-3* 4-1-4 showed a delay in flowering time when compared with *hos1-3*, indicating that the fusion protein was functional in the repression of flowering (Figure 7E). Subsequently, we grew 35S:HOS1-GFP/*hos1-3* 4-1-4 transgenic plants at 22°C under both continuous light and dark and analyzed GFP fluorescence in root cells by confocal microscopy. As shown in Figures 7A to 7C, HOS1-GFP was clearly targeted to the nucleus; whereas the fluorescence signal could be detected throughout the whole organelle, a significant fraction was localized to the nuclear envelope, independently of the light growing conditions. These results are in agreement with recent observations implicating HOS1 as an interactor of RNA export factor 1 (RAE1) nucleoporin (Tamura et al., 2010). Moreover, the nuclear localization of HOS1-GFP is also consistent with the results of the BiFC assay described above (Figure 6B) and with the detection of CO and other HOS1 targets in the nucleus (Valverde et al., 2004; Dong et al., 2006a).

Given the described interaction between CO and HOS1 (Figure 6) and because CO acts in the phloem companion cells to activate *FT* transcription (An et al., 2004), we tested whether HOS1 may also regulate flowering when specifically expressed in phloem tissue. Expression of *HOS1* under the control of the phloem companion cell-specific *SUCROSE H⁺ SYMPORTER2* (*SUC2*) promoter (Imlau et al., 1999) in *hos1* mutant plants delayed their flowering time and caused partial complementation of the early-flowering phenotype of *hos1* mutant (Figures 7D and 7E). By contrast, expression of *HOS1* under the shoot apical meristem specific promoter of the *KNOTTED-LIKE FROM ARABIDOPSIS THALIANA1* (*KNAT1*) gene (Lincoln et al., 1994) in *hos1* mutant plants did not alter their flowering time (Figures 7D and 7E), demonstrating that *HOS1* expression is required in the

Figure 6. (continued).

coimmunoprecipitated CO protein and input. Antibodies against ubiquitin recognized, in the same blot, a higher molecular mass band (asterisk) corresponding to an ubiquitinated CO form (elution HC, Bottom). Controls included input (1/50) from HC and H samples as well as column flow-through and washes. Protein markers are shown on the right.

(D) Noninvasive *in vivo* luciferase imaging of 35S:CO-LUC 6-2 and 35S:CO-LUC 6-2/*hos1-3* seedlings. Pictures show 7-d-old seedlings grown in LDs 3 h after the lights are on. At this time, more CO-LUC protein accumulates in *hos1* mutant (below right) than in the wild type (below left).

(E) Quantification of the luciferase activity in 35S:CO-LUC 6-2 (blue bars) and 35S:CO-LUC 6-2/*hos1-3* (gray bars) seedlings expressed as LUC counts per second (LCPS) in serial dilutions of fresh tissue in Steadylite Plus Reagent (mg/mL). Error bars represent SD.

(F) Immunoblot showing CO protein levels during a 24-h time course in nuclear extracts from Col and *hos1-3* plants grown under LDs. Numbers above each lane represent hours after dawn that the sample was harvested. Histone H3 was used as a loading control. Relative quantification of each band compared with the control is expressed below the top panel (α -CO).

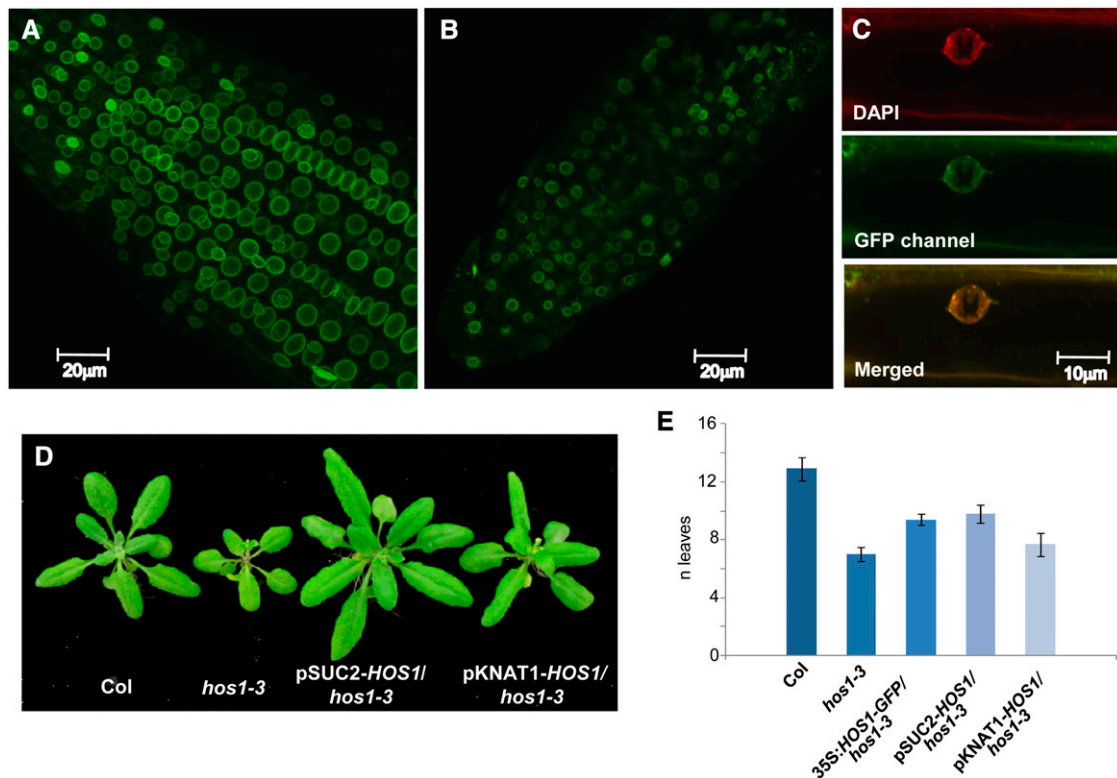


Figure 7. HOS1 Is a Nuclear-Localized Protein That Is Required in the Phloem to Regulate Photoperiodic Flowering.

Localization of HOS1-GFP in the root cells of 10-d-old *35S:HOS1-GFP/hos1-3* plants analyzed under confocal microscopy.

(A) Plants grown under continuous light.

(B) Plants grown in darkness.

(C) A representative nuclear image of a light-grown seedling showing 4',6-diamidino-2-phenylindole staining (DAPI; Top), GFP fluorescence (Middle), and the merge of both images (Bottom).

(D) Tissue-specific expression of *HOS1* in phloem companion cells and in the shoot apical meristem of *hos1* transgenic plants. Flowering time phenotype of Col, *hos1-3*, *SUC2:HOS1/hos1-3*, and *KNAT1:HOS1/hos1-3* plants in LDs.

(E) Quantification of flowering time of Col, *hos1-3*, *35S:HOS1-GFP/hos1-3*, *SUC2:HOS1/hos1-3*, and *KNAT1:HOS1/hos1-3* plants grown in LD conditions. Total number of leaves was scored in ~10 plants and is represented as mean ± SD.

phloem companion cells, where *CO* is expressed, to repress flowering.

HOS1 Interacts Synergistically with COP1 in the Control of Flowering Time

COP1 E3 ubiquitin ligase is involved in the degradation of CO protein during the night (Jang et al., 2008; Liu et al., 2008b). However, CO degradation in the morning occurs independently of COP1 (Jang et al., 2008), and for this reason, we speculate that HOS1 may be involved in this process. In our conditions, *cop1-4* mutants flowered dramatically earlier than wild-type and *hos1* plants under SDs. However, under LDs, *cop1-4* mutants flowered earlier than Col but later than *hos1* plants (Figure 8A, Table 1). To test the effect on flowering time of abolishing the activity of both HOS1 and COP1, we combined *hos1* and *cop1* mutations. Interestingly, the *hos1-3 cop1-4* double mutant flowered earlier than both parents in LDs and SDs, displaying the same number of leaves in both photoperiodic conditions (Figure 8A, Table 1).

This result indicates that the combination of both mutations renders a plant with a complete loss of photoperiod sensitivity and that *HOS1* and *COP1* genes are functionally related in the control of flowering time.

To further investigate the genetic interaction between *HOS1*, *COP1*, and *CO* genes in controlling *Arabidopsis* flowering time, a *hos1 cop1 co* triple mutant was generated and its flowering time was compared with that of *hos1 co* and *cop1 co* double mutants (Figure 8B, Table 1). Under LDs, the *hos1-3 co-10* and the *cop1-4 co-10* plants flowered with 12 and 10 leaves less than *co-10*, respectively, indicating that part of the early flowering phenotype of the *hos1-3* and *cop1-4* mutants in Col background occurs independently of CO. This result appears to be in contrast with the epistatic genetic relationship observed between *hos1-2* and *co-2* alleles in Ler background (Figure 4C, Table 1) and can be explained because the *hos1* mutation causes the downregulation of *FLC* expression (Figure 3B) and *FLC* is expressed at higher levels in Col than in Ler (Michaels and Amasino, 1999). Besides, the *hos1 cop1 co* triple mutant flowered with 15 leaves more than

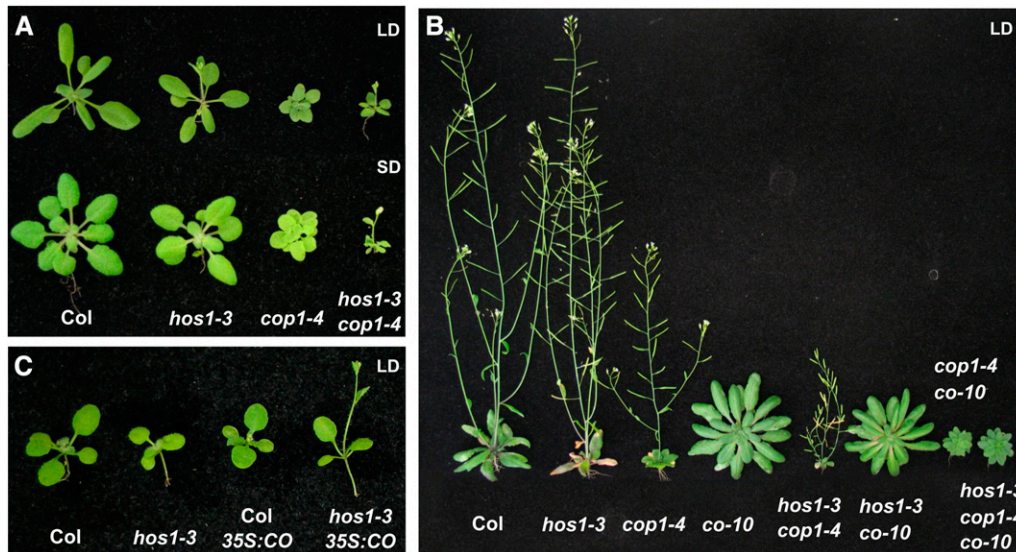


Figure 8. Genetic Interaction between *HOS1* and *COP1* in the Control of Flowering Time.

(A) Flowering time phenotype of *hos1-3 cop1-4* double mutant in LD (Top) and SD (Bottom) conditions.

(B) Flowering time phenotype of double and triple mutant combinations between *hos1-3 co-10 cop1-4* mutants grown in LD conditions.

(C) Comparison of flowering time phenotype between LD-grown Col and *hos1-3* plants bearing a *35S:CO* transgene.

the *hos1 cop1* double mutant under LD conditions, demonstrating that the *co* mutation notably delays the *hos1 cop1* early flowering phenotype in Col background. Interestingly, the *hos1 cop1 co* triple mutant formed six and nine leaves less than *hos1 co* and *cop1 co* double mutants, respectively (Figure 8B, Table 1), confirming the existence of a synergistic genetic interaction between *hos1* and *cop1*, even in the absence of *CO*.

Because *HOS1* seems to exert an effect as a negative regulator of *CO*, we tested whether the extremely early flowering of *35S:CO* plants (Simon et al., 1996) could be further accelerated by the *hos1-3* mutation. To test this hypothesis, the *35S:CO* transgene was introduced into wild-type Col and into *hos1-3* mutant plants. Although the number of leaves at flowering for both transgenic plants was very similar, we observed that the *hos1-3 35S:CO* plants bolted consistently earlier than the Col *35S:CO* (Figure 8C, Table 1), supporting a role for *HOS1* in repressing the promotion of flowering mediated by *CO*.

DISCUSSION

In many plants, changes in daylength regulate the transition from vegetative growth to flowering, and plants altered in the daylength-sensing mechanism cannot time flowering properly in natural environments (Wilczek et al., 2009). In this work, both genetic and molecular approaches demonstrate that *HOS1* is involved in the photoperiodic control of flowering time. The *esd6/hos1* mutant was identified through a screen designed to isolate early flowering mutants in *Arabidopsis*. The characterization of these mutants contributes to unveiling of the mechanisms of action of genes involved in the repression of the floral transition and suggests that a large number of genes participate in this

process (Pouteau et al., 2004; Jarillo and Piñeiro, 2011). In addition to precocious flowering, the *hos1* mutant showed pleiotropic alterations of leaf, flower, and root development, similar to those displayed by other early flowering mutants (Martin-Trillo et al., 2006; del Olmo et al., 2010).

In *Arabidopsis*, the flowering response due to changes in photoperiod relies on the interaction of light with the circadian clock-regulated rhythmic expression of *CO* (Suárez-López et al., 2001). Besides this transcriptional regulation, light-dependent regulation of *CO* protein stability has also been described (Valverde et al., 2004; Kim et al., 2008). We have demonstrated that *HOS1* is a nuclear-localized protein that acts in the phloem to repress flowering time (Figure 7) and that it is involved in regulating *CO* protein abundance in vivo (Figure 6), ensuring that *CO* activation of *FT* only occurs at the appropriate times of the day under inductive photoperiods in *Arabidopsis*. *HOS1* has been reported to work as an E3 ubiquitin ligase that mediates the degradation of the transcription factor *ICE1* (Dong et al., 2006a); here, we demonstrated that *CO* interacts in vitro and in planta with *HOS1* and that *CO* coimmunoprecipitates with *HOS1* in vivo (Figure 6). In addition, *hos1* mutation altered the *FT* expression pattern in LD, showing a peak of expression in the subjective morning (Figure 5C). These observations suggest that *HOS1* could mediate *CO* degradation during the daylight period through a mechanism involving ubiquitination and that the timing of *HOS1* activity is crucial to establish a photoperiodic flowering response (Figure 9). Both the genetic analysis between *CO* and *HOS1* genes (Figure 4) and the expression analyses of *CO* transcript and *CO* protein (Figures 5 and 6) support this hypothesis.

Other E3 ubiquitin ligases have been proposed to be involved in the control of flowering time (Cao et al., 2008; Vega-Sánchez et al., 2008; Park et al., 2010). In particular, *DAY NEUTRAL*

FLOWERING (DNF) and COP1 have been demonstrated to regulate the precise pattern of CO expression at the transcriptional and the posttranscriptional level, respectively (Jang et al., 2008; Liu et al., 2008b; Morris et al., 2010). DNF is an important regulator of the rhythm of CO expression, but it is not acting through the GI/FKF1/CDFs regulatory mechanism (Morris et al., 2010). Increased CO transcript in the *dnf* mutant around ZT 4-6 results in an earlier induction of FT under SDs (Morris et al., 2010). In addition, CO protein is degraded in the dark by the SUPPRESSOR OF PHYA-105 1 (SPA1)-COP1 complex (Laubinger et al., 2006; Jang et al., 2008; Liu et al., 2008b). Also, it has been demonstrated that the *Arabidopsis* CULLIN4 E3 RING ligase bound to Damaged DNA Binding protein 1 (DDB1) interacts with SPA1-COP1 complex to regulate flowering time (Chen et al., 2010). We have demonstrated that *HOS1* also interacts genetically with *COP1* in the photoperiodic control of flowering time (Figure 8A). Interestingly, *hos1 cop1* double mutants are completely insensitive to photoperiod, and *co* mutations notably delay the early flowering phenotype of the *hos1 cop1* double mutant (Figure 8B). This can be interpreted as HOS1 and COP1 being functionally related proteins in the control of flowering time, regulating CO abundance during the day and in the night, respectively (Figure 9). This is consistent with the observation that the absence of both E3 ubiquitin ligases renders plants unable to distinguish between LDs and SDs. It has been pro-

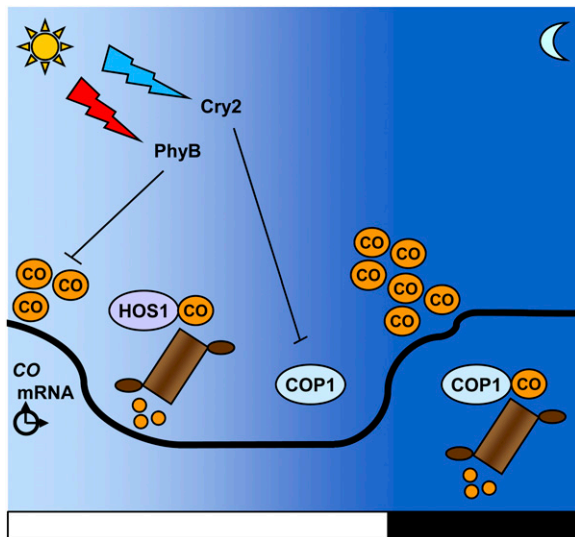


Figure 9. Model for HOS1 Function in the Photoperiodic Control of Flowering Time.

CO transcription depends primarily on the circadian clock (thick black line). In the evening, the degradation of CDFs by the GI/FKF1 complex allows CO transcript levels to increase, and CO protein accumulates due to a photoreceptor-mediated repression of COP1. At this time, CO can promote FT expression and induce flowering. During the night, COP1 activity causes rapid degradation of CO protein by the ubiquitination/26S proteasome system. In the daylight period, HOS1 is required to degrade CO. Additional data will be necessary to establish the possible involvement of HOS1 in the mechanism of CO degradation mediated by phyB that has been proposed to operate in the morning.

posed that a phyB-dependent mechanism occurring early in the day may promote CO degradation as well, but the E3 ubiquitin ligase(s) involved in this process remains to be identified (Valverde et al., 2004; Jang et al., 2008). Our data are consistent with HOS1 playing a crucial role in preventing increased CO protein levels and FT expression during early hours of the day. Further analyses will be required to establish the possible participation of HOS1 in the proposed phyB-dependent mechanism of CO proteolysis.

The ability to respond to photoperiod enables plants to anticipate variations in environmental conditions that can be predicted to occur periodically each year. In northern latitudes, shortening daylength in autumn is coupled with decreasing temperatures, while longer days are typically associated with warm temperatures. In addition to repressing the floral transition, HOS1 was previously described as a negative regulator of cold signal transduction (Lee et al., 2001). This suggests that HOS1 might function as an integrative link for both responses, allowing plants to discriminate the duration of the day by regulating CO abundance and to respond to cold temperatures by regulating CBF (for *C-repeat binding factors*) expression through ICE1 degradation (Dong et al., 2006a). Several lines of evidence point to the existence of overlapping pathways for controlling cold stress and flowering time responses in *Arabidopsis* (Yoo et al., 2007; Seo et al., 2009). The characterization of several mutants altered in cold acclimation responses has uncovered a role of the corresponding genes in flowering time control. The *hos9* and *sensitive to freezing6 (sfr6)* mutants show a late flowering phenotype, while the *long vegetative phase1 (lov1)* mutant is early flowering (Zhu et al., 2004; Yoo et al., 2007; Knight et al., 2008). These three genes regulate the expression of cold-inducible genes independently of CBFs, and both *LOV1* and *SFR6* control flowering time through the photoperiod pathway. Other mutants, such as *low expression of osmotically responsive genes4 (los4)* and *atnup160*, display an early flowering phenotype and altered CBF expression levels (Gong et al., 2005; Dong et al., 2006b). Moreover, *co* and *gi* photoperiod pathway mutants show altered tolerance to freezing temperatures (Cao et al., 2005; Yoo et al., 2007), and *fve* mutant flowers late and shows increased expression of *FLC* and *CBF* genes (Kim et al., 2004). It has been proposed that in warm late spring, *SOC1* downregulates CBFs expression and promotes flowering, but in cold early spring or fall, induction of *FLC* expression by the CBFs delays flowering and confers cold resistance to the plant (Seo et al., 2009). Besides regulating CO stability, *HOS1* controls *FLC* expression (Figure 3B) (Lee et al., 2001), which is also repressed by prolonged exposure to cold temperatures (Amasino, 2010). The positive effect of *HOS1* on *FLC* expression appears to be independent of the vernalization pathway (Bond et al., 2011) (see Supplemental Table 2 online) and is still uncharacterized. Taken together, these results suggest that HOS1, among other genes, may participate in the photoperiod and temperature signal crosstalk, integrating information coming from both pathways and facilitating a proper response to changing environmental conditions. Thus, this E3 ubiquitin ligase is proposed to integrate both environmental signals, specifically targeting for degradation key factors involved in the regulation of each response. Further studies will be necessary for an in-depth

understanding of how these pathways modulate each other's activity to optimize plant adaptation.

METHODS

Genetic Stocks and Growth Conditions

Arabidopsis thaliana mutant seed stocks used were in *Ler*, *Col*, and C24 genetic backgrounds and were obtained from the ABRC of Ohio State University (Columbus, OH), the Nottingham Arabidopsis Stock Centre (NASC) in the UK, and personal donations. C24 accession and mutant *hos1-1* seeds were kindly provided by Jian-Kang Zhu (Lee et al., 2001). The monogenic mutants used in this work were described previously: *fca-1*, *ft-1*, *co-2*, and *gi-3* (Koorneef, 1991); *fve-3* (Ausin et al., 2004); *flc-3* (Michaels and Amasino, 1999); *phyB-1* (Reed et al., 1993); *fha-1* (Guo et al., 1998); *vrn1-2 fca-1* (Levy et al., 2002); *vin3-4 FRI* Sf-2 (Sung and Amasino, 2004); *fld-1* (He et al., 2003); *siz1-2* (Miura et al., 2005); *fkf1-1* (Nelson et al., 2000); *cop1-4* (Deng et al., 1991); *co-10* (Laubinger et al., 2006); *soc1-1* (Samach et al., 2000); and the *Col FRI* Sf-2 line was described by Lee and Amasino (1995).

Plants were grown in plastic pots containing a mixture of substrate and vermiculite (3:1) or in MS (Murashige and Skoog) medium supplemented with 1% (w/v) Suc and 0.8% (w/v) agar for *in vitro* culture. Controlled environmental conditions were provided in growth chambers at 22°C and 70% relative humidity. Plants were illuminated with cool-white fluorescent lights (~120 μmol m⁻² s⁻¹). LD conditions consisted of 16 h of light followed by 8 h of darkness; SD conditions consisted of 8 h of light followed by 16 h of darkness.

Phenotypic Analysis

Total leaf number was scored as the number of leaves in the rosette (excluding cotyledons) plus the number of leaves in the inflorescence at the time of opening of the first flower (Koorneef, 1991). Cauline, adult, and juvenile leaves were scored independently. Rosette leaves lacking abaxial trichomes were considered as juvenile leaves (Telfer et al., 1997). Data are shown as mean ± SD.

Root length was measured at different developmental stages in seedlings grown in MS medium supplemented with 1% (w/v) Suc and 1% (w/v) plant agar in Petri dishes placed vertically.

Total chlorophyll content was calculated as described by Moran (1982).

Map-Based Cloning of *esd6* Mutation and Molecular Characterization of the *hos1* Alleles

A mapping population was generated by crossing the *esd6* mutant, in *Ler* background, and a *Col* wild-type plant. The analysis of 550 early flowering plants with several polymorphic molecular markers (see Supplemental Table 1 online) located the *esd6* mutation to the upper arm of chromosome 2, between markers C005 and T517. Mutations *hos1-1*, in C24 background, *hos1-2*, in *Ler* background, and *hos1-4*, in *Col* background, generate premature stop codons in the seventh, fifth, and first exon of the *HOS1* locus, respectively. The T-DNA insertion mutant *hos1-3*, isolated in *Col* background, was obtained from the NASC (SALK_069312).

Genetic Analysis

Double mutants were constructed by crossing the monogenic *hos1* mutants with lines carrying the mutations *flc-3*, *fca-1*, *fve-3*, *fld-1*, *siz1-2*, *fha-1*, *gi-3*, *co-2*, *co-10*, *cop1-4*, *fkf1-1*, *ft-1*, *soc1-1*, *vrn1-2*, or *vin3-4*. Double mutants were isolated from selfed F2 progeny using molecular markers. A derived cleaved-amplified polymorphic sequences marker was designed for the *hos1-2* mutation (PCR amplification using 5'-TTTTTACATGGCCGGTTCAGATC-3' and 5'-GCAATGTAATGTGAA-

ACTAGCGCA-3' primers followed by *Bgl*II digestion). For the *hos1-3* mutation, we used 5'-GGTTTCTGGACCGCATATTC-3', 5'-GGCTTCTGACCAGAGAGTGT-3', and the SALK LB1 primer. *hos1-3* was also crossed with lines carrying the *FRI* Sf-2 allele (Lee and Amasino, 1995) and the 35S:CO transgene (Simon et al., 1996).

Expression Analysis

Total RNA was isolated using TRIzol (Invitrogen-Gibco), and RT-PCR was performed in a range of DNA concentrations demonstrated to be quantitative. Amplified DNA was electrophoresed and transferred to nylon membranes (Martin-Trillo et al., 2006). For RT-PCR analysis, the *HOS1*-specific primers 5'-TTGCTCTATTGCGTTTGT-3' and 5'-TCAAATTGGGGAA-GAAGTTATG-3' were designed to amplify the N-terminal part of the *HOS1* coding region. The *FLC*, *CO*, *FT*, and *SOC1* primers used were described elsewhere (Piñeiro et al., 2003; Lázaro et al., 2008). *UBIQUITIN10* (*UBQ10*) was used as a loading control in these experiments. Detection was done using radioactively labeled specific probes. Q-PCR analyses were performed using FastStart Universal SYBR Green Master (Roche) and protocols and primers already described for analyzing the expression of *CO*, *FT*, *SOC1*, and *ACTIN2* (*ACT*) genes (Chiang et al., 2009; Morris et al., 2010).

In Vitro Pull-Down Assays

The pMAL and the pMAL-HOS1 constructs were expressed in *Escherichia coli* BL21 Rosetta strain and the proteins, MBP or MBP-HOS1, were purified on amylose resin (New England Biolabs). *In vitro* transcription/translation CO reactions were performed with the TNT Quick Coupled Transcription/Translation System (Promega) in the presence of [³⁵S]Met (Amersham Biosciences). For pull-down assays, 1 μg of MBP or MBP-HOS1 bound to beads was incubated with 15 μL of the TNT reaction in 200 μL of binding buffer containing 50 mM HEPES, pH 7.4, 1 mM EDTA, 150 mM NaCl, 10% (v/v) glycerol, 0.1% (v/v) Tween 20, and 0.5 mM DTT (Dong et al., 2006a). The mixture was incubated at room temperature for 1 h and then washed five times with washing buffer (50 mM Tris, pH 7.5, 150 mM NaCl, and 0.2% [v/v] Nonidet P-40). Samples were boiled in the presence of Laemmli buffer and analyzed by SDS-PAGE followed by autoradiography.

BiFC Studies

HOS1 and *CO* complete open reading frame were cloned in pYFN43 and pYFC43 vectors to produce *HOS1* fused to the N-terminal part of YFP (YFN-HOS1) and *CO* fused to the C-terminal part of the YFP (YFC-CO). These constructs were introduced into *Agrobacterium tumefaciens* strain C58C1. Five-week-old tobacco (*Nicotiana benthamiana*) or 3-week-old *Arabidopsis* Nossen (No-0) plants were leaf inoculated with YFC-CO and YFN-HOS1, the negative control pairs (YFC-CO coexpressed with YFN-AKINβ and YFC-AKIN10 with YFN-HOS1), or a positive control (amino and carboxy parts of AKINβ and AKIN10 SNF1-related kinases; Ferrando et al., 2001), following protocols previously described (Voinnet et al., 2003). Fluorescent interactions were visualized under a Leica TCS SP2 confocal microscope set at 550 nm. Images were analyzed employing Leica LCS Lite software.

Nuclear Protein Extraction and Immunological Experiments

Nuclei were isolated from *Arabidopsis* seedlings that were grown on MS plates for 2 weeks and then frozen. Plants were ground with mortar and pestle in the presence of liquid nitrogen and 30 mL of nuclei isolation buffer containing 50 mM MES-KOH, pH 8.0, 1 mM EDTA, pH 8.0, 30% (v/v) glycerol, 5% (w/v) Suc, 50 mM KCl, 10 mM MgCl₂, 10 mM PMSF, 0.1% (v/v) Triton X-100, and plant protease inhibitor cocktail (Sigma-Aldrich). The

slurry was filtered through 100- μ m mesh and centrifuged sequentially at 6,000 rpm for 20 min, 5,000 rpm for 10 min, and 4,000 rpm for 10 min in a Beckman Avanti J-26 XP centrifuge at 4°C in a JA-25.50 rotor, with the supernatant discarded at each step and the pellets resuspended in the same nuclei isolation buffer. The final pellet was resuspended in 1.5 mL of the same buffer omitting the detergent and centrifuged at 2,000g in a microfuge at 4°C. For immunoblot experiments, the nuclei-enriched preparation was disrupted in the presence of 6 M guanidine chlorhydrate with circular stirring at 4°C, sonicated in a Brandson sonifier set at 10 W, and centrifuged at 20,000g for 10 min in a microfuge at 4°C. The supernatant was precipitated with 90% (v/v) ethanol, recentrifuged at the same speed for 10 min, and washed three times in 90% (v/v) ethanol. The final pellet was dried and resuspended in Laemmli loading buffer and loaded into 4 to 12% (w/v) acrylamide gels. Immunoblots were performed as described before, using anti-CO antibodies (Valverde et al., 2004) and anti-H3 antibodies (AbCAM) as loading controls. Immunochemiluminescence signals were visualized and quantified using a ChemiDoc system (Bio-Rad).

For immunoprecipitation assays, nuclei-enriched preparations were suspended in high salt buffer (Sigma-Aldrich Cell-Lytic kit) including 1/100 Sigma-Aldrich plant protease inhibition cocktail for 4 h at 4°C and disrupted by sonication as before. Extracts were centrifuged at 20,000g in a microfuge at 4°C and the supernatant dialyzed against 50 mM MES, pH 8.0, 0.5% (v/v) Nonidet P-40, 10% (v/v) glycerol, 0.5 mM EDTA, pH 8, 1 mM PMSF, 1/100 Sigma-Aldrich plant protease inhibition cocktail, 1 mM DTT, and 10 mM β -mercapthoethanol for 4 h, at 4°C. Protein extracts (100 μ g) were incubated with 50 μ L of anti-GFP-Trap-A slurry (Chromotek) in the presence of 0.5 mM MG132 proteasome inhibitor at 4°C overnight, and proteins were processed following the instructions of the manufacturer. Eluted samples were run on a 10% (w/v) acrylamide/bis-acrylamide SDS-PAGE gel and immunoblots performed employing anti-CO and anti-ubiquitin antibodies as described before (Valverde et al., 2004).

LUC Activity Assays

A 35S:CO-LUC construct was transformed in Col plants and homozygous lines were established. Several independent transgenic plants exhibiting early flowering phenotype were selected, and one representative line was crossed with *hos1-3* plants. For noninvasive *in vivo* LUC imaging, 10-d-old Col and *hos1-3* seedlings harboring the 35S:CO-LUC construct were grown in MS plates and sprayed with 100 μ M luciferin (Biotium) 3 h after dawn. The imaging system consisted of the C2400-32 Photon Counting I-CCD video camera (Hamamatsu Photonics) mounted in a dark chamber. Image acquisition and processing were performed with Wasabi software provided by the camera manufacturer.

Quantification of LUC activity was assayed on seedlings grown in the same conditions described above with a MicroBeta TriLux luminometer (Perkin-Elmer). Seedlings were ground in liquid nitrogen and resuspended in Steadylite Plus Reagent (Perkin-Elmer). The luciferase activity was measured as a mean of three independent experiments and expressed as luciferase counts per second in serial dilutions of fresh tissue in Steadylite Plus Reagent (mg/mL).

Subcellular Localization of HOS1

hos1-3 mutant plants were transformed with a 35S:HOS1-GFP construct, and the selected transgenic plants were grown in MS medium supplemented with 1% (w/v) Suc and 1% (w/v) plant agar in Petri dishes placed vertically. Ten-day-old transgenic plants grown under continuous light or dark conditions were analyzed by confocal microscopy (Zeiss LSM 710). The 4',6-diamidino-2-phenylindole staining of the nuclei was done at a final concentration of 10 μ g/mL with 0.1% (v/v) Tween 20.

Accession Numbers

Sequence data from this article can be found in the Arabidopsis Genome Initiative or GenBank/EMBL databases under the following accession numbers: *ESD6/HOS1* (At2g39810), *CO* (At5g15840), *SOC1* (At2g45660), *FT* (At1g65480), *FLC* (At5g10140), *TSF* (At4g20370), *GI* (At1g22770), *AS1* (At2g37630), *FKF1* (At1g68050), *ZTL* (At5g57360), *LKP2* (At2g18915), *COP1* (At2g32950), *CRY2* (At1g04400), *PHYB* (At2g18790), *FCA* (At4g16280), *FVE* (At2g19520), *VRN1* (At3g18990), *VIN3* (At5g57380), *FRI* (At4g00650), *FLD* (At3g10390), *SIZ1* (At5g60410), *UBQ10* (At4g05320), *ACT2* (At3g18780), *ICE1* (At3g26744), *AKIN β 2* (At4g16360), *AKIN10* (At3g01090), *RAE1* (At1g80670), *DNF* (At3g19140), *SPA1* (At2g46340), *CUL4* (At5g46210), *DDB1A* (At4g05420), *SFR6* (At4g04920), *LOV1* (At2g02450), *LOS4* (At3g53110), and *At NUP160* (At1g33410).

Supplemental Data

The following materials are available in the online version of this article.

Supplemental Figure 1. Flower, Silique, and Root Length Measurement in *Ler* and *esd6*.

Supplemental Figure 2. Map-Based Cloning of *ESD6*.

Supplemental Figure 3. Sequence Comparison of *Arabidopsis* HOS1 (At HOS1) with the HOS1 Orthologs.

Supplemental Figure 4. Expression Analysis of Different Flowering Time Genes over a 24-h Time Course in *Ler* and *hos1-2*.

Supplemental Figure 5. *FT* Expression Analysis in LD-Grown Col and *hos1-3*.

Supplemental Table 1. Polymorphic Molecular Markers Used for *esd6* Mapping.

Supplemental Table 2. Flowering Time of *hos1* and Mutations in Vernalization Pathway Genes.

Supplemental Table 3. Flowering Time of Transgenic Plants Bearing a CO-LUC Construct.

ACKNOWLEDGMENTS

We thank Israel Ausin (Centro Nacional de Biotecnología, Consejo Superior de Investigaciones Científicas, Madrid, Spain) for isolating the *esd6* mutant, Rafael Catalá (Centro de Investigaciones Biológicas, Consejo Superior de Investigaciones Científicas, Madrid, Spain) for providing a Gateway-compatible *HOS1* full-length cDNA, Julio Salinas (Centro de Investigaciones Biológicas, Consejo Superior de Investigaciones Científicas) for granting the access to the luciferase imaging system, Pablo González-Melendi (Centro de Biotecnología y Genómica de Plantas, Instituto Nacional de Investigación y Tecnología Agraria y Alimentaria-Universidad Politécnica de Madrid) for technical support with confocal microscopy, and Juan C. del Pozo and members of his lab (Centro de Biotecnología y Genómica de Plantas, Instituto Nacional de Investigación y Tecnología Agraria y Alimentaria-Universidad Politécnica de Madrid) for helpful discussions. pYFN43 and pYFC43 vectors, and SNF1 protein kinase constructs, used as positive controls in the BiFC assays, were kindly provided by Alejandro Ferrando (Instituto de Biología Molecular y Celular de Plantas, Valencia, Spain). C24 and *hos1-1* mutant seeds, as well as a *HOS1* expression construct in the pMAL vector, were kindly provided by Jian-Kang Zhu (University of California, Riverside, CA). The 35S:CO construct, the plasmids containing the *SUC2* and *KNAT1* promoters, and *co-10 cop1-4* seeds were kindly donated by George Coupland (Max Planck Institute, Cologne, Germany), and the 35S:CO-LUC plasmid was kindly provided by Hong-Quan Yang (Shanghai Institute for Biological Sciences, Chinese Acad-

emy of Science, Shanghai, China). This work was supported by Grant BIO2008-00351 to J.A.J., Grant BIO2007-61215 to M.P., Grants CSD2007-00057 and BIO2010-15589 to J.A.J. and M.P., and Grants BIO2007-61837 and BIO2010-16027 to F.V. from the Spanish Ministerio de Ciencia e Innovación.

AUTHOR CONTRIBUTIONS

M.P. and J.A.J. designed the research. A.L. performed all the experiments except for the immunoblot assays, the BiFC studies, and the coimmunoprecipitation experiments, which were performed by F.V. All the authors analyzed data and wrote the article.

Received December 23, 2010; revised February 1, 2012; accepted February 16, 2012; published March 9, 2012.

REFERENCES

- Adrian, J., Farrona, S., Reimer, J.J., Albani, M.C., Coupland, G., and Turck, F. (2010). *cis*-Regulatory elements and chromatin state coordinately control temporal and spatial expression of *FLOWERING LOCUS T* in *Arabidopsis*. *Plant Cell* **22**: 1425–1440.
- Amasino, R. (2010). Seasonal and developmental timing of flowering. *Plant J.* **61**: 1001–1013.
- An, H., Roussot, C., Suárez-López, P., Corbesier, L., Vincent, C., Piñero, M., Hepworth, S., Mouradov, A., Justin, S., Turnbull, C., and Coupland, G. (2004). *CONSTANS* acts in the phloem to regulate a systemic signal that induces photoperiodic flowering of *Arabidopsis*. *Development* **131**: 3615–3626.
- Ausín, I., Alonso-Blanco, C., Jarillo, J.A., Ruiz-García, L., and Martínez-Zapater, J.M. (2004). Regulation of flowering time by FVE, a retinoblastoma-associated protein. *Nat. Genet.* **36**: 162–166.
- Bond, D.M., Dennis, E.S., and Finnegan, E.J. (2011). The low temperature response pathways for cold acclimation and vernalization are independent. *Plant Cell Environ.* **34**: 1737–1748.
- Cao, S., Ye, M., and Jiang, S. (2005). Involvement of *GIGANTEA* gene in the regulation of the cold stress response in *Arabidopsis*. *Plant Cell Rep.* **24**: 683–690.
- Cao, Y., Dai, Y., Cui, S., and Ma, L. (2008). Histone H2B monoubiquitination in the chromatin of *FLOWERING LOCUS C* regulates flowering time in *Arabidopsis*. *Plant Cell* **20**: 2586–2602.
- Corbesier, L., Vincent, C., Jang, S., Fornara, F., Fan, Q., Searle, I., Giakountis, A., Farrona, S., Gissot, L., Turnbull, C., and Coupland, G. (2007). FT protein movement contributes to long-distance signaling in floral induction of *Arabidopsis*. *Science* **316**: 1030–1033.
- Chen, H., Huang, X., Gusmaroli, G., Terzaghi, W., Lau, O.S., Yanagawa, Y., Zhang, Y., Li, J., Lee, J.H., Zhu, D., and Deng, X.W. (2010). *Arabidopsis* CULLIN4-damaged DNA binding protein 1 interacts with CONSTITUTIVELY PHOTOMORPHOGENIC1-SUPPRESSOR OF PHYA complexes to regulate photomorphogenesis and flowering time. *Plant Cell* **22**: 108–123.
- Chiang, G.C., Barua, D., Kramer, E.M., Amasino, R.M., and Donohue, K. (2009). Major flowering time gene, *flowering locus C*, regulates seed germination in *Arabidopsis thaliana*. *Proc. Natl. Acad. Sci. USA* **106**: 11661–11666.
- del Olmo, I., López-González, L., Martín-Trillo, M.M., Martínez-Zapater, J.M., Piñero, M., and Jarillo, J.A. (2010). *EARLY IN SHORT DAYS 7 (ESD7)* encodes the catalytic subunit of DNA polymerase epsilon and is required for flowering repression through a mechanism involving epigenetic gene silencing. *Plant J.* **61**: 623–636.
- de Montaigu, A., Tóth, R., and Coupland, G. (2010). Plant development goes like clockwork. *Trends Genet.* **26**: 296–306.
- Deng, X.W., Caspar, T., and Quail, P.H. (1991). *cop1*: A regulatory locus involved in light-controlled development and gene expression in *Arabidopsis*. *Genes Dev.* **5**: 1172–1182.
- Deshaies, R.J., and Joazeiro, C.A. (2009). RING domain E3 ubiquitin ligases. *Annu. Rev. Biochem.* **78**: 399–434.
- Dong, C.H., Agarwal, M., Zhang, Y., Xie, Q., and Zhu, J.K. (2006a). The negative regulator of plant cold responses, HOS1, is a RING E3 ligase that mediates the ubiquitination and degradation of ICE1. *Proc. Natl. Acad. Sci. USA* **103**: 8281–8286.
- Dong, C.H., Hu, X., Tang, W., Zheng, X., Kim, Y.S., Lee, B.H., and Zhu, J.K. (2006b). A putative *Arabidopsis* nucleoporin, AtNUP160, is critical for RNA export and required for plant tolerance to cold stress. *Mol. Cell. Biol.* **26**: 9533–9543.
- Ferrando, A., Koncz-Kálmán, Z., Farràs, R., Tiburcio, A., Schell, J., and Koncz, C. (2001). Detection of *in vivo* protein interactions between Snf1-related kinase subunits with intron-tagged epitope-labelling in plants cells. *Nucleic Acids Res.* **29**: 3685–3693.
- Fornara, F., de Montaigu, A., and Coupland, G. (2010). SnapShot: Control of flowering in *Arabidopsis*. *Cell* **141**: 550, 550e1–550e2.
- Fornara, F., Panigrahi, K.C., Gissot, L., Sauerbrunn, N., Rühl, M., Jarillo, J.A., and Coupland, G. (2009). *Arabidopsis* DOF transcription factors act redundantly to reduce *CONSTANS* expression and are essential for a photoperiodic flowering response. *Dev. Cell* **17**: 75–86.
- Gong, Z., Dong, C.H., Lee, H., Zhu, J., Xiong, L., Gong, D., Stevenson, B., and Zhu, J.K. (2005). A DEAD box RNA helicase is essential for mRNA export and important for development and stress responses in *Arabidopsis*. *Plant Cell* **17**: 256–267.
- Guo, H., Yang, H., Mockler, T.C., and Lin, C. (1998). Regulation of flowering time by *Arabidopsis* photoreceptors. *Science* **279**: 1360–1363.
- He, Y., Michaels, S.D., and Amasino, R.M. (2003). Regulation of flowering time by histone acetylation in *Arabidopsis*. *Science* **302**: 1751–1754.
- Imaizumi, T. (2010). *Arabidopsis* circadian clock and photoperiodism: time to think about location. *Curr. Opin. Plant Biol.* **13**: 83–89.
- Imaizumi, T., Schultz, T.F., Harmon, F.G., Ho, L.A., and Kay, S.A. (2005). FKF1 F-box protein mediates cyclic degradation of a repressor of *CONSTANS* in *Arabidopsis*. *Science* **309**: 293–297.
- Imlau, A., Truernit, E., and Sauer, N. (1999). Cell-to-cell and long-distance trafficking of the green fluorescent protein in the phloem and symplastic unloading of the protein into sink tissues. *Plant Cell* **11**: 309–322.
- Jackson, S.D. (2009). Plant responses to photoperiod. *New Phytol.* **181**: 517–531.
- Jaeger, K.E., and Wigge, P.A. (2007). FT protein acts as a long-range signal in *Arabidopsis*. *Curr. Biol.* **17**: 1050–1054.
- Jang, S., Marchal, V., Panigrahi, K.C., Wenkel, S., Soppe, W., Deng, X.W., Valverde, F., and Coupland, G. (2008). *Arabidopsis* COP1 shapes the temporal pattern of CO accumulation conferring a photoperiodic flowering response. *EMBO J.* **27**: 1277–1288.
- Jang, S., Torti, S., and Coupland, G. (2009). Genetic and spatial interactions between *FT*, *TSF* and *SVP* during the early stages of floral induction in *Arabidopsis*. *Plant J.* **60**: 614–625.
- Jarillo, J.A., and Piñero, M. (2011). Timing is everything in plant development. The central role of floral repressors. *Plant Sci.* **181**: 364–378.
- Jin, J.B., et al. (2008). The SUMO E3 ligase, *AtSIZ1*, regulates flowering by controlling a salicylic acid-mediated floral promotion pathway and through affects on *FLC* chromatin structure. *Plant J.* **53**: 530–540.
- Johanson, U., West, J., Lister, C., Michaels, S., Amasino, R., and Dean, C. (2000). Molecular analysis of *FRIGIDA*, a major determinant

- of natural variation in *Arabidopsis* flowering time. *Science* **290**: 344–347.
- Kim, H.J., Hyun, Y., Park, J.Y., Park, M.J., Park, M.K., Kim, M.D., Kim, H.J., Lee, M.H., Moon, J., Lee, I., and Kim, J.** (2004). A genetic link between cold responses and flowering time through *FVE* in *Arabidopsis thaliana*. *Nat. Genet.* **36**: 167–171.
- Kim, S.Y., Yu, X., and Michaels, S.D.** (2008). Regulation of *CONSTANS* and *FLOWERING LOCUS T* expression in response to changing light quality. *Plant Physiol.* **148**: 269–279.
- Knight, H., Thomson, A.J., and McWatters, H.G.** (2008). Sensitive to freezing6 integrates cellular and environmental inputs to the plant circadian clock. *Plant Physiol.* **148**: 293–303.
- Kobayashi, Y., and Weigel, D.** (2007). Move on up, it's time for change — Mobile signals controlling photoperiod-dependent flowering. *Genes Dev.* **21**: 2371–2384.
- Koornneef, M.** (1991). Isolation of higher plant developmental mutants. *Symp. Soc. Exp. Biol.* **45**: 1–19.
- Koornneef, M., Alonso-Blanco, C., Peeters, A.J., and Soppe, W.** (1998). Genetic control of flowering time in *Arabidopsis*. *Annu. Rev. Plant Physiol. Plant Mol. Biol.* **49**: 345–370.
- Kumimoto, R.W., Zhang, Y., Siefers, N., and Holt III, B.F.** (2010). NF-YC3, NF-YC4 and NF-YC9 are required for *CONSTANS*-mediated, photoperiod-dependent flowering in *Arabidopsis thaliana*. *Plant J.* **63**: 379–391.
- Laubinger, S., Marchal, V., Le Gourrierec, J., Wenkel, S., Adrian, J., Jang, S., Kulajta, C., Braun, H., Coupland, G., and Hoecker, U.** (2006). *Arabidopsis* SPA proteins regulate photoperiodic flowering and interact with the floral inducer *CONSTANS* to regulate its stability. *Development* **133**: 3213–3222. Erratum. *Development* **133**: 4608.
- Lázaro, A., Gómez-Zambrano, A., López-González, L., Piñeiro, M., and Jarillo, J.A.** (2008). Mutations in the *Arabidopsis* *SWC6* gene, encoding a component of the SWR1 chromatin remodelling complex, accelerate flowering time and alter leaf and flower development. *J. Exp. Bot.* **59**: 653–666.
- Lee, H., Xiong, L., Gong, Z., Ishitani, M., Stevenson, B., and Zhu, J.K.** (2001). The *Arabidopsis* *HOS1* gene negatively regulates cold signal transduction and encodes a RING finger protein that displays cold-regulated nucleocytoplasmic partitioning. *Genes Dev.* **15**: 912–924.
- Lee, I., and Amasino, R.M.** (1995). Effect of vernalization, photoperiod, and light quality on the flowering phenotype of *Arabidopsis* plants containing the *FRIGIDA* gene. *Plant Physiol.* **108**: 157–162.
- Levy, Y.Y., Mesnage, S., Mylne, J.S., Gendall, A.R., and Dean, C.** (2002). Multiple roles of *Arabidopsis* *VRN1* in vernalization and flowering time control. *Science* **297**: 243–246.
- Lincoln, C., Long, J., Yamaguchi, J., Serikawa, K., and Hake, S.** (1994). A *knotted1*-like homeobox gene in *Arabidopsis* is expressed in the vegetative meristem and dramatically alters leaf morphology when overexpressed in transgenic plants. *Plant Cell* **6**: 1859–1876.
- Liu, H., Yu, X., Li, K., Klejnot, J., Yang, H., Lisiero, D., and Lin, C.** (2008a). Photoexcited CRY2 interacts with CIB1 to regulate transcription and floral initiation in *Arabidopsis*. *Science* **322**: 1535–1539.
- Liu, L.J., Zhang, Y.C., Li, Q.H., Sang, Y., Mao, J., Lian, H.L., Wang, L., and Yang, H.Q.** (2008b). COP1-mediated ubiquitination of *CONSTANS* is implicated in cryptochrome regulation of flowering in *Arabidopsis*. *Plant Cell* **20**: 292–306.
- Martin-Trillo, M., Lázaro, A., Poethig, R.S., Gómez-Mena, C., Piñeiro, M.A., Martínez-Zapater, J.M., and Jarillo, J.A.** (2006). *EARLY IN SHORT DAYS 1 (ESD1)* encodes ACTIN-RELATED PROTEIN 6 (AtARP6), a putative component of chromatin remodelling complexes that positively regulates *FLC* accumulation in *Arabidopsis*. *Development* **133**: 1241–1252.
- Michaels, S.D.** (2009). Flowering time regulation produces much fruit. *Curr. Opin. Plant Biol.* **12**: 75–80.
- Michaels, S.D., and Amasino, R.M.** (1999). *FLOWERING LOCUS C* encodes a novel MADS domain protein that acts as a repressor of flowering. *Plant Cell* **11**: 949–956.
- Miura, K., Jin, J.B., Lee, J., Yoo, C.Y., Stirn, V., Miura, T., Ashworth, E.N., Bressan, R.A., Yun, D.J., and Hasegawa, P.M.** (2007). SIZ1-mediated sumoylation of ICE1 controls *CBF3/DREB1A* expression and freezing tolerance in *Arabidopsis*. *Plant Cell* **19**: 1403–1414.
- Miura, K., Rus, A., Sharkhuu, A., Yokoi, S., Karthikeyan, A.S., Raghobama, K.G., Baek, D., Koo, Y.D., Jin, J.B., Bressan, R.A., Yun, D.J., and Hasegawa, P.M.** (2005). The *Arabidopsis* SUMO E3 ligase SIZ1 controls phosphate deficiency responses. *Proc. Natl. Acad. Sci. USA* **102**: 7760–7765.
- Moran, R.** (1982). Formulae for determination of chlorophyllous pigments extracted with n,n-dimethylformamide. *Plant Physiol.* **69**: 1376–1381.
- Morris, K., Thornber, S., Codrai, L., Richardson, C., Craig, A., Sadanandom, A., Thomas, B., and Jackson, S.** (2010). *DAY NEUTRAL FLOWERING* represses *CONSTANS* to prevent *Arabidopsis* flowering early in short days. *Plant Cell* **22**: 1118–1128.
- Nelson, D.C., Lasswell, J., Rogg, L.E., Cohen, M.A., and Bartel, B.** (2000). *FKF1*, a clock-controlled gene that regulates the transition to flowering in *Arabidopsis*. *Cell* **101**: 331–340.
- Park, B.S., Eo, H.J., Jang, I.C., Kang, H.G., Song, J.T., and Seo, H.S.** (2010). Ubiquitination of LHY by SINAT5 regulates flowering time and is inhibited by DET1. *Biochem. Biophys. Res. Commun.* **398**: 242–246.
- Piñeiro, M., Gómez-Mena, C., Schaffer, R., Martínez-Zapater, J.M., and Coupland, G.** (2003). *EARLY BOLTING IN SHORT DAYS* is related to chromatin remodeling factors and regulates flowering in *Arabidopsis* by repressing *FT*. *Plant Cell* **15**: 1552–1562.
- Pouteau, S., Ferret, V., Gaudin, V., Lefebvre, D., Sabar, M., Zhao, G., and Prunus, F.** (2004). Extensive phenotypic variation in early flowering mutants of *Arabidopsis*. *Plant Physiol.* **135**: 201–211.
- Reed, J.W., Nagpal, P., Poole, D.S., Furuya, M., and Chory, J.** (1993). Mutations in the gene for the red/far-red light receptor phytochrome B alter cell elongation and physiological responses throughout *Arabidopsis* development. *Plant Cell* **5**: 147–157.
- Roux, F., Touzet, P., Cuguen, J., and Le Corre, V.** (2006). How to be early flowering: an evolutionary perspective. *Trends Plant Sci.* **11**: 375–381.
- Samach, A., Onouchi, H., Gold, S.E., Ditta, G.S., Schwarz-Sommer, Z., Yanofsky, M.F., and Coupland, G.** (2000). Distinct roles of *CONSTANS* target genes in reproductive development of *Arabidopsis*. *Science* **288**: 1613–1616.
- Sawa, M., Nusinow, D.A., Kay, S.A., and Imaizumi, T.** (2007). FKF1 and GIGANTEA complex formation is required for day-length measurement in *Arabidopsis*. *Science* **318**: 261–265.
- Searle, I., He, Y., Turck, F., Vincent, C., Fornara, F., Kröber, S., Amasino, R.A., and Coupland, G.** (2006). The transcription factor *FLC* confers a flowering response to vernalization by repressing meristem competence and systemic signaling in *Arabidopsis*. *Genes Dev.* **20**: 898–912.
- Seo, E., Lee, H., Jeon, J., Park, H., Kim, J., Noh, Y.S., and Lee, I.** (2009). Crosstalk between cold response and flowering in *Arabidopsis* is mediated through the flowering-time gene *SOC1* and its upstream negative regulator *FLC*. *Plant Cell* **21**: 3185–3197.
- Serrano, G., Herrera-Palau, R., Romero, J.M., Serrano, A., Coupland, G., and Valverde, F.** (2009). Chlamydomonas *CONSTANS* and the evolution of plant photoperiodic signaling. *Curr. Biol.* **19**: 359–368.
- Simon, R., Igeño, M.I., and Coupland, G.** (1996). Activation of floral meristem identity genes in *Arabidopsis*. *Nature* **384**: 59–62.
- Song, Y.H., Lee, I., Lee, S.Y., Imaizumi, T., and Hong, J.C.** (2012). *CONSTANS* and *ASYMMETRIC LEAVES 1* complex is involved in the

- induction of *FLOWERING LOCUS T* in photoperiodic flowering in *Arabidopsis*. *Plant J.* **69**: 332–342.
- Suárez-López, P., Wheatley, K., Robson, F., Onouchi, H., Valverde, F., and Coupland, G.** (2001). *CONSTANS* mediates between the circadian clock and the control of flowering in *Arabidopsis*. *Nature* **410**: 1116–1120.
- Sung, S., and Amasino, R.M.** (2004). Vernalization in *Arabidopsis thaliana* is mediated by the PHD finger protein VIN3. *Nature* **427**: 159–164.
- Tamura, K., Fukao, Y., Iwamoto, M., Haraguchi, T., and Hara-Nishimura, I.** (2010). Identification and characterization of nuclear pore complex components in *Arabidopsis thaliana*. *Plant Cell* **22**: 4084–4097.
- Telfer, A., Bollman, K.M., and Poethig, R.S.** (1997). Phase change and the regulation of trichome distribution in *Arabidopsis thaliana*. *Development* **124**: 645–654.
- Tiwari, S.B., et al.** (2010). The flowering time regulator *CONSTANS* is recruited to the *FLOWERING LOCUS T* promoter via a unique *cis*-element. *New Phytol.* **187**: 57–66.
- Turck, F., Fornara, F., and Coupland, G.** (2008). Regulation and identity of florigen: *FLOWERING LOCUS T* moves center stage. *Annu. Rev. Plant Biol.* **59**: 573–594.
- Valverde, F.** (2011). *CONSTANS* and the evolutionary origin of photoperiodic timing of flowering. *J. Exp. Bot.* **62**: 2453–2463.
- Valverde, F., Mouradov, A., Soppe, W., Ravenscroft, D., Samach, A., and Coupland, G.** (2004). Photoreceptor regulation of *CONSTANS* protein in photoperiodic flowering. *Science* **303**: 1003–1006.
- Vega-Sánchez, M.E., Zeng, L., Chen, S., Leung, H., and Wang, G.L.** (2008). *SPIN1*, a K homology domain protein negatively regulated and ubiquitinated by the E3 ubiquitin ligase *SPL11*, is involved in flowering time control in rice. *Plant Cell* **20**: 1456–1469.
- Vierstra, R.D.** (2009). The ubiquitin-26S proteasome system at the nexus of plant biology. *Nat. Rev. Mol. Cell Biol.* **10**: 385–397.
- Voinnet, O., Rivas, S., Mestre, P., and Baulcombe, D.** (2003). An enhanced transient expression system in plants based on suppression of gene silencing by the p19 protein of tomato bushy stunt virus. *Plant J.* **33**: 949–956.
- Wenkel, S., Turck, F., Singer, K., Gissot, L., Le Gourrierec, J., Samach, A., and Coupland, G.** (2006). *CONSTANS* and the CCAAT box binding complex share a functionally important domain and interact to regulate flowering of *Arabidopsis*. *Plant Cell* **18**: 2971–2984.
- Wilczek, A.M., et al.** (2009). Effects of genetic perturbation on seasonal life history plasticity. *Science* **323**: 930–934.
- Yoo, S.K., Chung, K.S., Kim, J., Lee, J.H., Hong, S.M., Yoo, S.J., Yoo, S.Y., Lee, J.S., and Ahn, J.H.** (2005). *CONSTANS* activates *SUPPRESSOR OF OVEREXPRESSION OF CONSTANS 1* through *FLOWERING LOCUS T* to promote flowering in *Arabidopsis*. *Plant Physiol.* **139**: 770–778.
- Yoo, S.Y., Kim, Y., Kim, S.Y., Lee, J.S., and Ahn, J.H.** (2007). Control of flowering time and cold response by a NAC-domain protein in *Arabidopsis*. *PLoS ONE* **2**: e642.
- Yu, J.W., et al.** (2008). *COP1* and *ELF3* control circadian function and photoperiodic flowering by regulating *GI* stability. *Mol. Cell* **32**: 617–630.
- Zhu, J., Shi, H., Lee, B.H., Damsz, B., Cheng, S., Stirm, V., Zhu, J.K., Hasegawa, P.M., and Bressan, R.A.** (2004). An *Arabidopsis* homeodomain transcription factor gene, *HOS9*, mediates cold tolerance through a *CBF*-independent pathway. *Proc. Natl. Acad. Sci. USA* **101**: 9873–9878.
- Zuo, Z., Liu, H., Liu, B., Liu, X., and Lin, C.** (2011). Blue light-dependent interaction of *CRY2* with *SPA1* regulates *COP1* activity and floral initiation in *Arabidopsis*. *Curr. Biol.* **21**: 841–847.